



On the mechanical behavior of two directional symmetrical functionally graded beams under moving load

Alaa A. Abdelrahman · Mohamed Ashry · Amal E. Alshorbagy · Waleed S. Abdallah

Received: 3 February 2021 / Accepted: 8 May 2021 / Published online: 30 May 2021
© The Author(s), under exclusive licence to Springer Nature B.V. 2021

Abstract This article presents a different polynomial interpolation function based dynamic finite element model to study and analyze the mechanical behavior of bidirectional functionally graded beams under moving load. To improve the mechanical behavior of the functionally graded beam, material properties are assumed to be symmetrically distributed throughout the axial and transverse directions. The first order shear deformation theory is employed to incorporate the transverse shear strain. To overcome the shear locking phenomena with satisfying all true kinematic constraints and no need to assume new strain field, five noded beam element with ten degrees of freedom and different polynomial interpolation functions is used. Cubic polynomial interpolation functions are assumed for the transverse deflection while quadratic polynomials are used for both axial and rotational displacements. Equations of motion are developed using the virtual displacement principle. Finite elements stiffness, mass matrices and force vector are derived in explicit forms. The unconditionally stable Newmark technique is employed for the transient time response. The developed procedure is checked and compared with the available results and

an excellent agreement is observed. The applicability of the developed numerical procedure is demonstrated and discussed. Effects of the geometrical, material characteristics, and the moving load speed on the mechanical behavior are investigated and discussed. Obtained results are supportive for the design and manufacturing of bidirectional functionally graded beam structures.

Keywords Dynamic finite element · Shear locking · Different polynomial interpolation functions · Moving load · Two directional symmetrical functionally graded material · Dynamic behavior

1 Introduction

Functionally graded materials, FGMs are new kind of composites, which possess smooth continuous variation of microstructure and mechanical characteristics without internal boundaries and sharp interfacial stress variations, (Elishakoff et al. 2015; Nie and Zhong 2010). In these materials, the properties are continuously varied in a given direction, (Malekzadeh and Heydarpour 2012). FGMs are commonly made of ceramic and metal mixture. The ceramic materials are characterized by its good thermal resistance as well as anti-oxidant behavior. On the other hand, metallic materials have excellent strength and superior fracture toughness, (Jha et al. 2013). Due to large applicability

A. A. Abdelrahman (✉) · M. Ashry · A. E. Alshorbagy · W. S. Abdallah
Mechanical Design & Production Department, Faculty of Engineering, Zagazig University,
P.O. Box 44519, Zagazig, Egypt
e-mail: alaaabouahmed@gmail.com

of the FGMs such as automotive industry, nuclear structures, and aircraft industry, serious attempts were performed by many researchers to study and analyze the mechanical behavior of this modern category of composite materials, (Kieback et al. 2003; Naebe and Shirvanimoghaddam 2016; Sarathchandra et al. 2018). Many attempts had been performed to combine metal-ceramic mixture in FGMS, Japanese researchers succeeded to develop a combination between metal and ceramic with thermal gradation 1000 k through thickness of 10 mm, (Esen et al. 2021). Interests of studying and analyzing the FGMs have several aspects such as distribution of the material properties and deformation theories, (Liew et al. 2015) or their applicability such as beam, plate, and shell structures under thermal, mechanical or thermo-mechanical analysis, (static, buckling, free and forced vibration) (Eltaher et al. 2014; Attia and Abdelrahman 2018).

Regarding the property graduation point of view, the FGMs properties can be varied through one or several spatial directions by controlling the volume fraction of the constituents, (Ghatage et al. 2020). Many mathematical forms are used to express the volume fraction distribution throughout a given direction of FGMs. Both the power law and exponential functions are the most common mathematical models used to express the properties distribution, (Mohammadian 2021). Many efforts have been done to relate the volume fraction at any point to the magnitude of the property such as rule of mixture or Mori–Tanaka Scheme which assuming no interaction between phases or applying Tamura-Tomota-Ozawa (TTO) model given by Tamura that consider for the bonding effect (Jha et al. 2013; Nikbakht et al. 2019). Other researchers give more interest in the response of FGMs so they assumed an arbitrary distribution of properties for studying without regarding to the way they could achieve such gradation, (Sofiyev 2019). Yongdong et al. (2005) investigated stresses in functionally graded beams based on effective principal axes method.

On the other hand, considering the deformation theories point of view, the well-known Euler–Bernoulli beam theory (EBBT) is the oldest and simplest beam theory that described beam deformation, Li and Batra (2013). In thick beams, which possess transverse shear strain EBBT was unable to efficiently describe the mechanical behavior of such types of beams. Shear deformation beam theories are

required for effective investigation of the mechanical behavior of thick beams. The first order shear deformation theory, developed by Timoshenko and Ehrenfest and known as Timoshenko beam theory (TBT), is considered as the simplest theory in which the shear deformation effect was incorporated through the analysis of beams, Elishakoff (2020). In this theory, the shear effect is considered by assuming that the edges after deformation is not perpendicular to each other anymore but still straight. To achieve that assumption, the transverse deformation and rotation have to be independent of each other with C^0 continuity, Elishakoff (2019). Applying the TBT to detect the mechanical behavior of slender beams and thin plates using the same interpolation function for the transverse deflection and rotation, shear locking (SL) phenomena is appeared. In such case a nonzero transverse shear strain is detected, (Oñate 2013).

Many techniques have been developed to overcome shear locking (SL) in the analyses of slender beams and thin plates. Some of the most commonly applied techniques are the reduced integration techniques; Lin et al. (2020), the assumed shear strain field technique, The discrete Kirchhoff methodology, and the mixed interpolation of tensorial components (MITC) (Oñate 2013; Wang et al. 2014; Lin et al. 2020). Although these techniques are efficient to remove shear locking, the accuracy of the finite elements may be reduced. Seeking for simple and accurate locking free finite element model, formulations based on interpolation functions that embody interdependency between bending and shear deformation have been developed, [Reddy (1997); Mukherjee and Prathap(2001); Edem (2006)]. For efficient investigation of nonlinear behavior of structures and alleviate shear and membrane locking phenomena that commonly occurred in shell structures, finite element based on isogeometric analysis was developed on higher order interpolation function bases (Liu et al. 2020; Liu and Jeffers 2017, 2018).

Another weakness of TBT is coming out from the straightness of edges assumption that lead to constant transverse shear stress distribution through thickness and to overcome that problem there is a need to apply shear correction factor, (Mena et al. 2012; Sina et al. 2009; Wei et al. (2012)). To eliminate the weakness encountered in TBT due to straightness assumption, the second order shear deformation beam theory was

proposed, (Khoshgoftar 2019). A more precise beam theory is the third order shear theory which allow parabolic shear strain through thickness and verify the zero-shear stress condition at the upper and lower surface of beam, (Reddy 1984; Thai and Vo (2012; Maia et al. 2020; Attia and Mohamed, 2020). More comprehensive shear deformation theories have been discussed in many research articles (Touratier 1991; Soldatos 1992; Karama et al. 2003; Carrera 2003; Abdelrahman and Eltahir 2020; Bouazza and Zenkour 2020; Boussoula et al. 2020; Jiang et al. 2020; Nguyen et al. (2020a, b); Qin et al. 2020; Shafei et al. 2020; Van Do et al. 2020).

Considering the applications point of view, recently, analysis of the static as well as dynamic behavior of functionally graded beams (FGBs) have been studied through many beam's theories for various type of material gradation function, (Esen 2020a; Le et al. 2020; Xie et al. 2020a). For unidirectional functionally graded materials, (Sankar 2001) investigated the static mechanical behavior of unidirectional functionally graded beam (UFGB) based on EBBT. Applying the EBBT, the free vibration behavior of axially functionally graded beam (AFGB) with non-uniform cross section was investigated by (Huang and Li 2010) while the free vibration behavior of TBT was analyzed by (Huang et al. 2013).

Considering the variation of the material properties throughout the axial and thickness directions, (Al-shorbagy et al. 2011) presented the free vibration characteristic for FGBs based on EBBT. (Lee and Lee 2017) developed exact transfer matrix method for analyzing the free vibration response of FGBs. (Şimşek 2010) performed the fundamental frequency analysis of FGB using the first-order and different higher-order shear deformation beam theories. (Jing et al. 2016) combined TBT with finite volume method to analysis the static and free vibration response of FGM. (Nguyen et al. 2013) have developed the first order shear deformation theory to obtain the static and free vibration solution of one dimension FGBs. (Kadoli et al. 2008). Studied the static behavior of metal-ceramic FGBs under ambient temperature using higher order beam theory (RBT). (Pradhan and Chakraverty 2015) Introduced generalized power-law exponent based shear deformation beam theory (PESDBT) to analysis the free vibration response of FGB with power-law material variation through the thickness. Atmane et al. (2017) investigated effect of

thickness stretching and porosity on mechanical behavior of functionally graded beams. Within the framework of the improved third-order shear deformable theory, Xie et al. (2020b) investigated the nonlinear vibration and dynamic response.

For more improvement of the functionally graded material characteristics, two directional material gradation become necessary for many applications, (Tlidji et al. 2019). Applying different beam theories, (Karamanli 2017) has introduced a static bending solution of two directional functionally graded beams with power law variation. (Pydah and Sabale 2017) studied the static behavior of curved bi-directional FGB using EBBT. Using both power and exponential laws for FGMs, (Huang and Ouyang 2020) have introduced closed form solution for the static bending of two directional functionally graded Timoshenko beam FGTBs under various boundary and loading conditions. Applying the higher order shear deformation theory, (Huang 2020) analyzed both static and free vibration behaviors of two directional FGB. Based on the exponential gradation law, (Karamanli 2018) has studied the free vibration behavior of two direction FGBs using Reddy beam theory (RBT). Based on state space approach, (Deng and Cheng 2016) have studied the dynamic behavior of two direction FGBs based on TBT. Based on neural network-differential evolution approach, (Truong et al. 2020) developed an optimization technique for bidirectional functionally graded materials distribution to investigate the free vibration behavior of beams. (Lu and Chen 2020), studied the parametric dynamics of bidirectional functionally graded (BDFG) beams subjected to a time-dependent axial force. Based on finite element analysis. (Viet et al. 2020) Investigated the free vibration characteristics of sectioned unidirectional/bidirectional functionally graded material cantilever (Zhang et al. 2020a, b) proposed multifunctional nonlinear composite structure consisting of functionally graded beams and piezoelectric sheets for energy harvesting systems. Jamshidi et al. (2019) proposed an optimization procedure to achieve optimal post-buckling behavior of 2D functionally graded beams.

Regarding the functionally graded structures under moving loads, many attempts have been performed to study and analyze functionally graded beams and structural elements under moving loads. (Şimşek et al. 2012) investigated the dynamic behavior of

axially functionally graded EBBT subjected to moving load. In the context of finite element formulation, Esen et al. (2018) developed a finite element formulation to analyze the dynamic behavior of functionally graded Timoshenko beams under accelerating moving load. Applying Timoshenko beam hypothesis, (Nguyen et al. 2017) introduced the free vibration analysis of two directional FGB under moving load. Comparison between the dynamic behaviors of two directional functionally graded beams based on EBBT and TBT under moving load was performed by (Şimşek 2015). Wang et al. (2018) investigated vibration behavior of longitudinally moving sigmoid functionally graded material plates with porosities. (Nguyen et al. 2020a), investigated the dynamic behavior of a bidirectional functionally graded sandwich beam under non-uniform motion of a moving load. Based on higher order shear deformation beam theory, Wang et al. (2020) investigated the transient response of a sandwich porous beam uniformly distributed moving mass. Further readings on functionally graded beams under moving loads may be found in (Zhang and Liu, 2020; Esen (2019a, b, 2020a); Akbas et al. (2020), Özarpa and Esen 2020a, b, Ebrahimi et al. 2020).

Among these resources, there was no evidence of developing dynamic finite element model capable of investigating the static as well as the dynamic behavior of symmetrical functionally graded first order shear deformation beams under moving load considering the shear locking conditions. The present study aims to present a dynamic finite element model to study and analyze the mechanical behavior of bidirectional symmetrical functionally graded beams under moving loads. The first order shear deformation theory is adopted to incorporate the transverse shear strain effect. To avoid the shear locking effect, different polynomial interpolation functions technique is adopted based on five noded isoparametric finite elements. Thus zero shear strain condition for thin beams is satisfied with no need for assuming new strain field or eliminating any of the true kinematic constraints. The proposed numerical procedure is verified and compared. Static, free and forced vibration behaviors are investigated and analyzed. The rest of the manuscript is organized as follows:—The mathematical model is presented in Sect. 2. Section 3 aims to present the finite element formulation and solution procedure. In Sect. 4, the verification of the

proposed numerical procedure is presented. The numerical results and discussions are presented in Sect. 5. Finally, the concluding remarks are presented in Sect. 6.

2 Mathematical model

Consider a straight functionally graded beam of length L , uniform thickness h and width b as shown in Fig. 1. The material properties are assumed to be gradually changed in both thickness and length directions. According to the power law function, the symmetrical material distribution through thickness and length can be expressed as, Elishakoff et al. (2015):

$$P(x, z) = (P_1 - P_2) \left(\left| \frac{z}{h} \right| + 0.5 \right)^{r_z} \left(\left| \frac{x}{L} \right| + 0.5 \right)^{r_x} + P_2 \quad (1a)$$

where P is the property, $P_{1,2}$ are the reference properties, r_x and r_z are the gradation index through the length and thickness respectively.

Due to the graded properties of the beam material, the neutral axis at which zero normal stress is attained will not be coincided with mid plane axis and will be dislocated by distance d through z direction. Due to the dislocation of neutral axis from the mid-plane axis there will be axial displacement u_o associated with bending displacement θ , (Oñate 2013). The location of the neutral axis can be given by, (Eltaher et al. 2013)

$$d = \frac{\int_{-h/2}^{h/2} z E(x, z) dz}{\int_{-h/2}^{h/2} E(x, z) dz} \quad (1b)$$

For material with symmetrical distribution of the material properties along the mid-plane; the neutral axis dislocation is equal zero. Based on first order shear deformation theory, the displacement field can

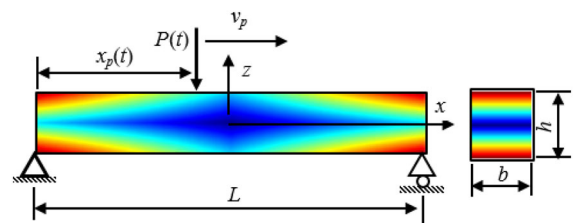


Fig. 1 Geometry of bidirectional functionally graded Beam under moving load

be expressed as, (Elishakoff (2019, 2020); Hu et al. 2020)

$$\begin{aligned} u(x, z, t) &= u_0(x, t) - (z - d)\theta(x, t), \\ w(x, z, t) &= w_0(x, t), v(x, z, t) = 0 \end{aligned} \tag{2}$$

where u_0 is the axial displacement, w_0 is the transverse displacement and θ is the cross-sections rotation. Based on the displacement field given by Eq. (2), the kinematic relations can be written as.

The axial and shear strain in matrix form can be defined by

$$\begin{aligned} \left\{ \begin{matrix} \varepsilon_x \\ \gamma_{xz} \end{matrix} \right\} &= \begin{bmatrix} 1 & -(z-d) & 0 \\ 0 & 0 & 1 \end{bmatrix} \left\{ \begin{matrix} \frac{\partial u_0(x, t)}{\partial x} \\ \frac{\partial \theta(x, t)}{\partial x} \\ \frac{\partial w_0(x, t)}{\partial x} - \theta(x, t) \end{matrix} \right\} \\ &= S\hat{\varepsilon} \end{aligned} \tag{3}$$

where $\frac{\partial u_0(x, t)}{\partial x}$ represent the beam elongation, $\frac{\partial \theta(x, t)}{\partial x}$ represent beam curvature and $\frac{\partial w_0(x, t)}{\partial x} - \theta(x, t)$ represent the beam transverse shear and all this component are represent the generalized strain vector $\hat{\varepsilon}$. The material constitutive relations for bidirectional functionally graded materials can be expressed as

$$\left\{ \begin{matrix} \sigma_x \\ \tau_{xz} \end{matrix} \right\} = \begin{bmatrix} E(x, z) & -(z-d)E(x, z) & 0 \\ 0 & 0 & k_z G(x, z) \end{bmatrix} \hat{\varepsilon} \tag{4}$$

where σ_x and τ_{xz} are the normal and shear components of Cauchy stress tensor; respectively. $E(x, z)$ and $G(x, z)$ are the elasticity and rigidity moduli of the bidirectional functionally graded materials; respectively. k_z is the shear correction factor. The balance of the internal forces is found by.

$$N = \int_A \sigma_x dA, M = - \int_A (z-d)\sigma_x dA, Q = \int_A \tau_{xz} dA \tag{5}$$

where N , M and Q are respectively the normal, bending and shear forces. By substituting with Eq. (4) into Eq. (5), and rewrite the forces in matrix form as,

$$\hat{\sigma} = \begin{Bmatrix} N \\ M \\ Q \end{Bmatrix} = \begin{bmatrix} D_a & D_{ab} & 0 \\ D_{ab} & D_b & 0 \\ 0 & 0 & D_s \end{bmatrix} \hat{\varepsilon} = \widehat{D}\hat{\varepsilon} \tag{6}$$

where D_a, D_b, D_{ab}, D_s are respectively the axial stiffness, bending stiffness, coupling axial-bending stiffness, and shear stiffness which can be given by, (Eltaher et al. 2014)

$$\begin{aligned} [D_a D_{ab} D_b] &= \int_A [1z z^2] E(x, z) dA \text{ and} \\ D_s &= \int_A k_z G(x, z) dA \end{aligned} \tag{7}$$

The strain energy of functionally graded Timoshenko beam given by, (Esen 2020b)

$$\begin{aligned} U &= \frac{1}{2} \iiint_{\Omega} (\sigma_{xx}\varepsilon_{xx} + \tau_{xz}\gamma_{xz}) d\Omega \\ &= \frac{1}{2} \int_0^L \left[D_a \left(\frac{\partial u_0(x, t)}{\partial x} \right)^2 - 2D_{ab} \left(\frac{\partial u_0(x, t)}{\partial x} \right) \left(\frac{\partial \theta(x, t)}{\partial x} \right) \right. \\ &\quad \left. + D_b \left(\frac{\partial \theta(x, t)}{\partial x} \right)^2 + \kappa_z D_s \left(\frac{\partial w_0(x, t)}{\partial x} - \theta(x, t) \right)^2 \right] dx \end{aligned} \tag{8}$$

The kinetic energy of functionally graded Timoshenko beam can be expressed as, (Özarpa and Esen 2020a, b)

$$\begin{aligned} T &= \frac{1}{2} \int_0^L \left[I_a \left\{ \left(\frac{\partial u_0(x, t)}{\partial t} \right)^2 + \left(\frac{\partial w_0(x, t)}{\partial t} \right)^2 \right\} \right. \\ &\quad \left. + I_b \left(\frac{\partial \theta(x, t)}{\partial t} \right)^2 - 2I_{ab} \left(\frac{\partial u_0(x, t)}{\partial t} \right) \left(\frac{\partial \theta(x, t)}{\partial t} \right) \right] dx \end{aligned} \tag{9}$$

where I_a, I_b, I_{ab} are respectively the inertia components of the functionally graded beam which can be expressed as, (Eltaher et al. 2014)

$$[I_a I_{ab} I_b] = \int_A [1z z^2] \rho(x, z) dA \tag{10}$$

The potential of the moving load (V) is simply given by, (Nguyen et al. 2017)

$$V = - \int_0^L P w_0(x, t) \delta(x_p - vt) dx \tag{11}$$

where $\delta(\cdot)$ is the Dirac delta function, and x is the abscissa, measured from the left end of the beam. Applying the virtual displacement principle as

$$\int_0^t (\delta T - \delta U - \delta V) dt = 0 \tag{12}$$

Evaluating the variations and performing the integral leads to the following dynamic equations of motion of functionally graded Timoshenko beam under moving load: -

$$I_a \frac{\partial^2 u_0(x, t)}{\partial t^2} - I_{ab} \frac{\partial^2 \theta(x, t)}{\partial t^2} = D_a \frac{\partial^2 u_0(x, t)}{\partial x^2} - D_{ab} \frac{\partial \theta(x, t)}{\partial x} \tag{13}$$

$$I_a \frac{\partial^2 w_0(x, t)}{\partial t^2} - P \delta(x_p - vt) = \kappa_z D_s \left[\frac{\partial^2 w_0(x, t)}{\partial x^2} + \frac{\partial \theta(x, t)}{\partial x} \right] \tag{14}$$

$$I_b \frac{\partial^2 \theta(x, t)}{\partial t^2} - I_{ab} \frac{\partial^2 u_0(x, t)}{\partial t^2} = D_b \frac{\partial^2 \theta(x, t)}{\partial x^2} - D_{ab} \frac{\partial^2 u_0(x, t)}{\partial x^2} + \kappa_z D_s \left[\frac{\partial w_0(x, t)}{\partial x} - \theta(x, t) \right] \tag{15}$$

3 Finite element formulation

3.1 Discretized finite element equation of motion

To seek for an efficient numerical tool to solve the dynamic equations of motion (13–15), the finite element is adopted. To derive the dynamic finite elements equilibrium equations, the virtual displacement principle is applied as, (Abdelrahman and El-Shafei 2020):

$$\delta(T + U - V) = 0 \tag{16}$$

where, T, U, V are respectively the variation, the total kinetic energy, the total strain energy, and the work done by the external forces. Substituting for the kinetic, strain energies and the work done, Eq. (16) can be expressed, (Nguyen et al. 2017):

$$\begin{aligned} & \delta \left(\frac{1}{2} \int_0^L \left[I_a \left\{ \left(\frac{\partial u_0(x, t)}{\partial t} \right)^2 + \left(\frac{\partial w_0(x, t)}{\partial t} \right)^2 \right\} \right. \right. \\ & \quad \left. \left. + I_b \left(\frac{\partial \theta(x, t)}{\partial t} \right)^2 - 2I_{ab} \left(\frac{\partial u_0(x, t)}{\partial t} \right) \left(\frac{\partial \theta(x, t)}{\partial t} \right) \right] dx \right) \\ & + \delta \left(\frac{1}{2} \int_0^L \left[D_a \left(\frac{\partial u_0(x, t)}{\partial x} \right)^2 - 2D_{ab} \left(\frac{\partial u_0(x, t)}{\partial x} \right) \left(\frac{\partial \theta(x, t)}{\partial x} \right) \right. \right. \\ & \quad \left. \left. + D_b \left(\frac{\partial \theta(x, t)}{\partial x} \right)^2 + \kappa_z D_s \left(\frac{\partial w_0(x, t)}{\partial x} - \theta(x, t) \right) \right] dx \right) \\ & - \delta \left(\int_0^L P w_0(x, t) \delta(x_p - vt) dx \right) = 0 \end{aligned} \tag{17}$$

To overcome the shear locking problem, five noded isoparametric element with ten degrees of freedom, shown in Fig. 2 and mixed shape function is adopted, (Baier-Saip et al. 2020). The displacement field can be interpolated as:

$$\begin{Bmatrix} u \\ w \end{Bmatrix} = \begin{bmatrix} 1 & -(z-d) & 0 \\ 0 & 0 & 1 \end{bmatrix} \begin{bmatrix} N_1 & 0 & 0 & 0 & N_2 & 0 & 0 & N_3 & 0 & 0 \\ 0 & 0 & N_1 & 0 & 0 & N_2 & 0 & 0 & 0 & N_3 \\ 0 & \bar{N}_1 & 0 & \bar{N}_2 & 0 & 0 & \bar{N}_3 & 0 & \bar{N}_4 & 0 \end{bmatrix} \{a\} \tag{18}$$

where the quadratic shape functions, used for the axial and rotational degrees of freedom, u_o, θ are given by, (Oñate 2013)

$$\begin{aligned} N_1(\xi) &= \frac{1}{2} \xi(\xi - 1), N_2(\xi) = (1 - \xi^2), N_3(\xi) \\ &= \frac{1}{2} \xi(\xi + 1) \end{aligned} \tag{19.a}$$

While cubic shape functions used for the transverse deflection, w_0 and given by

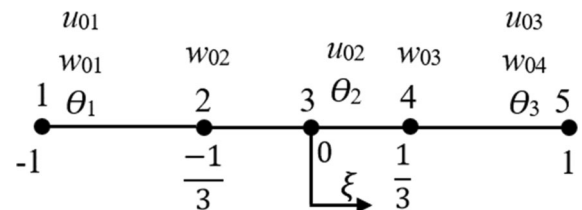


Fig. 2 five nodes beam element

$$\begin{aligned} \bar{N}_1(\xi) &= \frac{-9}{16} \left(\xi + \frac{1}{3}\right) \left(\xi - \frac{1}{3}\right) (\xi - 1), \\ \bar{N}_2(\xi) &= \frac{27}{16} (\xi + 1) \left(\xi - \frac{1}{3}\right) (\xi - 1), \\ \bar{N}_3(\xi) &= \frac{-27}{16} (\xi + 1) \left(\xi + \frac{1}{3}\right) (\xi - 1), \\ \bar{N}_4(\xi) &= \frac{9}{16} \left(\xi + \frac{1}{3}\right) \left(\xi - \frac{1}{3}\right) (\xi + 1) \end{aligned} \tag{19.b}$$

$$a^T = [u_{01} \quad w_{01} \quad \theta_1 \quad w_{02} \quad u_{02} \quad \theta_2 \quad w_{03} \quad u_{03} \quad w_{04} \quad \theta_3] \tag{19.c}$$

With ξ is the local coordinate system, $\xi = \frac{2}{l^e}(x - x_c)$, l^e is the element length, x_c is the coordinate of the element center. Based on the assumed displacement interpolation functions, the kinematic relations can be expressed as

$$\begin{Bmatrix} \varepsilon_x \\ \gamma_{xz} \end{Bmatrix} = \begin{bmatrix} 1 & -(z-d) & 0 \\ 0 & 0 & 1 \end{bmatrix} \begin{bmatrix} \frac{d\xi}{dx} \frac{dN_1}{d\xi} & 0 & 0 & 0 & \frac{d\xi}{dx} \frac{dN_2}{d\xi} & 0 & 0 & \frac{d\xi}{dx} \frac{dN_3}{d\xi} & 0 & 0 \\ 0 & 0 & \frac{d\xi}{dx} \frac{dN_1}{d\xi} & 0 & 0 & \frac{d\xi}{dx} \frac{dN_2}{d\xi} & 0 & 0 & 0 & \frac{d\xi}{dx} \frac{dN_3}{d\xi} \\ 0 & \frac{d\xi}{dx} \frac{d\bar{N}_1}{d\xi} & -N_1 & \frac{d\xi}{dx} \frac{d\bar{N}_2}{d\xi} & 0 & -N_2 & \frac{d\xi}{dx} \frac{d\bar{N}_3}{d\xi} & 0 & \frac{d\xi}{dx} \frac{d\bar{N}_4}{d\xi} & -N_3 \end{bmatrix} \{a\} \tag{20}$$

With $\frac{d\xi}{dx} = \frac{2}{l^e}$ Substituting Eqs. (6), (18), and (20) into Eq. (17), the variational form can be written as

$$\begin{aligned} &\frac{1}{2} \int_0^l \delta \dot{a}^T N^T C N \dot{a} dx + \frac{1}{2} \int_0^l \delta a^T B^T \hat{D} B a dx \\ &- \left[(P \times (N_w)_{atx=x_p}) \delta a + \int_0^l f N_w \delta a dx \right] \\ &= 0 \end{aligned} \tag{21}$$

where C is the equivalent inertia components of the functionally graded material, which is given by

$$\begin{aligned} [C] &= \int_A \rho(x, z) s^T s dA \\ &= \int_A \rho(x, z) \begin{bmatrix} 1 & 0 \\ -(z-d) & 0 \\ 0 & 1 \end{bmatrix} \begin{bmatrix} 1 & -(z-d) & 0 \\ 0 & 0 & 1 \end{bmatrix} dA \\ &= \begin{bmatrix} I_a & -I_{ab} & 0 \\ -I_{ab} & I_b & 0 \\ 0 & 0 & I_a \end{bmatrix} \end{aligned} \tag{22}$$

While x_p presents the position of the moving load, for steady state velocity, $x_p = v_p \times t$, N_w is the shape function vector for the transverse deflection, w , which can be expressed as

$$N_w = [0 \quad \bar{N}_1 \quad 0 \quad \bar{N}_2 \quad 0 \quad 0 \quad \bar{N}_3 \quad 0 \quad \bar{N}_4 \quad 0]^T \tag{23}$$

Evaluating the variations in Eq. (21) and recalling Gauss quadrature to evaluate the integrals, the following discretized form of the dynamic equation of motion is obtained:-

$$\sum_{e=1}^{NE} [M^e] \{\ddot{a}\} + \sum_{e=1}^{NE} [K^e] \{a\} = \{Q\} \tag{24}$$

where NE are the total number of finite elements, and $[M^e]$, $[K^e]$, and Q are respectively the element mass and stiffness matrices and the external force vector, which are obtained as

$$\begin{aligned} [M^e] &= \frac{l^e}{2} \int_{-1}^1 N^T C N d\xi, [K^e] \\ &= \frac{l^e}{2} \int_{-1}^1 B^T \hat{D} B d\xi \text{ and } Q \\ &= P \times (N_w)_{atx=x_p} + \frac{l^e}{2} \int_{-1}^1 f N_w d\xi \end{aligned} \tag{25}$$

3.2 Solution methodology

To study and analyze the mechanical behavior of the functionally graded Timoshenko beam, both static and dynamic behavior are investigated. The static behavior is investigated by neglecting the inertia effects and assuming that the load is applied gradually with no shocks. Thus, the governing equilibrium equations is simplified into the following form:

$$\sum_{e=1}^{NE} [K^e] \{a\} = \{Q\} \tag{26}$$

On the other hand, the free vibration behavior is investigated by neglecting the effect of the external applied load leading to the following equation of motion:

$$\sum_{e=1}^{NE} [M^e] \{\ddot{a}\} + \sum_{e=1}^{NE} [K^e] \{a\} = 0 \tag{27}$$

Assuming harmonic response, then the unknown displacement, velocity, and acceleration can be expressed as

$$a = Ae^{i w_n t}, \dot{a} = Ai w_n e^{i w_n t}, \text{ and } \ddot{a} = -A w_n^2 e^{i w_n t} \tag{28}$$

By substituting in the discretized Eq. (27), the free vibration behavior can be obtained by solving the following eigen value problem: -

$$[K - w_n^2 M] \{A\} = 0 \tag{29}$$

where w_n represent the natural frequency and $\{A\}$ is the vibration mode vector.

Finally, the forced vibration response is investigated by solving the dynamic equation of motion, Eq. (24) using implicit integration techniques. The most common scheme for implicit time integration is the Newmark scheme in which assume linear variation of acceleration through time step as below, (Borst et al. 2012):

$$\ddot{a}^{t+\Delta t} = \ddot{a}^t + \Delta t((1 - \gamma)\ddot{a}^t + \gamma\ddot{a}^{t+\Delta t}) \tag{30}$$

$$a^{t+\Delta t} = a^t + \Delta t \dot{a}^t + \frac{1}{2} \Delta t^2 ((1 - 2\beta)\ddot{a}^t + 2\beta\ddot{a}^{t+\Delta t}) \tag{31}$$

where β and γ are parameter determine the stability of the system. For unconditionally stability of linear system

$$2\beta \geq \gamma \geq \frac{1}{2} \tag{32}$$

The acceleration can be expressed as below by rearranging the previous equation for displacement

$$\ddot{a}^{t+\Delta t} = \frac{1}{\beta \Delta t^2} \left(a^{t+\Delta t} - a^t - \Delta t \dot{a}^t - \frac{1}{2} \Delta t^2 \ddot{a}^t (1 - 2\beta) \right) \tag{33}$$

Recall equation of motion, Eq. (24):

$$M \ddot{a}^{t+\Delta t} + K a^{t+\Delta t} = Q(t) \tag{34}$$

By substitute with acceleration and displacement in equation of motion:

$$M \left(\frac{1}{\beta \Delta t^2} \left(a^{t+\Delta t} - a^t - \Delta t \dot{a}^t - \frac{1}{2} \Delta t^2 \ddot{a}^t (1 - 2\beta) \right) \right) + K a^{t+\Delta t} = Q(t)$$

$$\left[K + \frac{1}{\beta \Delta t^2} M \right] a^{t+\Delta t} = Q^{t+\Delta t} + M \left(\frac{a^t}{\beta \Delta t^2} + \frac{\dot{a}^t}{\beta \Delta t} + \ddot{a}^t \left(\frac{1}{2\beta} - 1 \right) \right) \tag{35}$$

where

$$[\widehat{K}] = \left[K + \frac{1}{\beta \Delta t^2} M \right] \tag{36}$$

$$\{\widehat{R}\} = Q^{t+\Delta t} + M \left(\frac{a^t}{\beta \Delta t^2} + \frac{\dot{a}^t}{\beta \Delta t} + \ddot{a}^t \left(\frac{1}{2\beta} - 1 \right) \right) \tag{37}$$

4 Verification of the developed procedure

Within this section, the developed numerical procedure is verified by comparing the obtained results with the available results in literature. Static as well as dynamic behaviors of bidirectional functionally graded beams are verified and compared. For all verification cases, the material properties distribution of the functionally graded material is graduated through the axial and transverse directions according to the following form:

Table 1 Dimensionless maximum transverse deflections of the SS and CS TDFG beam with the exponential-law gradient at $L/h = 5$

B_{CS}	r_z	r_x	0.2		0.4		0.6		0.8		1.0	
			Huang and Ouyang (2020)	Present	Huang and Ouyang (2020)	Present	Huang and Ouyang (2020)	Present	Huang and Ouyang (2020)	Present	Huang and Ouyang (2020)	Present
SS	0	17.1850	17.1850	15.5617	14.1134	14.1247	12.8198	12.8436	11.6626	11.6995	10.6263	10.6823
	0.2	15.5520	15.5520	14.0829	12.7723	12.7824	11.6015	11.6231	10.5543	10.5877	9.6164	9.6671
	0.4	14.0784	14.0784	12.7485	11.5620	11.5712	10.5021	10.5216	9.5541	9.5842	8.7050	8.7508
	0.6	12.7480	12.7480	11.5438	10.4694	10.4777	9.5096	9.5272	8.6511	8.6783	7.8821	7.9235
	0.8	11.5464	11.5464	10.4557	9.4825	9.4900	8.6130	8.6290	7.8354	7.8599	7.1388	7.1762
CS	0	8.2911	8.2921	7.6310	7.0305	7.0313	6.4912	6.4867	5.9974	5.9961	5.5530	5.5476
	0.2	7.5014	7.5022	6.9041	6.3607	6.3615	5.8728	5.8687	5.4260	5.4248	5.0238	5.0190
	0.4	6.7855	6.7863	6.2451	5.7534	5.7542	5.3120	5.3083	4.9079	4.9067	4.5439	4.5395
	0.6	6.1366	6.1375	5.6479	5.2030	5.2037	4.8036	4.8002	4.4381	4.4370	4.1086	4.1047
	0.8	5.5487	5.5495	5.1067	4.7041	4.7048	4.3429	4.3397	4.0122	4.0112	3.7141	3.7105
1.0	5.0161	5.0169	4.6163	4.2520	4.2528	3.9254	3.9225	3.6263	3.6253	3.3565	3.3532	

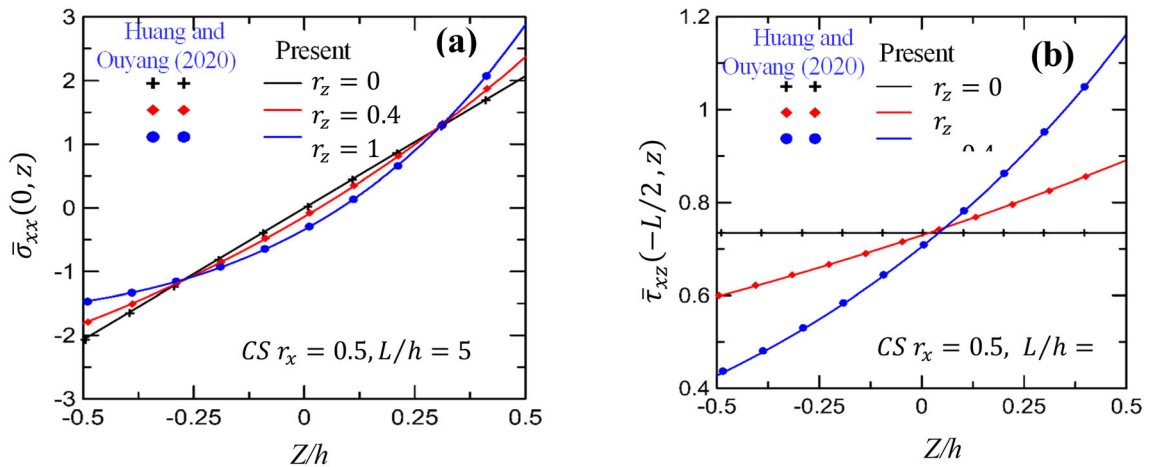


Fig. 3 Dimensionless stress through the thickness for CS TDFG beam

$$P(x, z) = P_0 e^{r_x(\frac{x}{L}+0.5)+r_z(\frac{z}{h}+0.5)} \tag{38}$$

where P is the property, P_0 is the reference property, r_x and r_z are the gradation index through the axial and transverse directions, respectively.

4.1 Static behavior

The static analysis is performed on a beam under uniformly distributed load of intensity, q_0 with reference material properties given by $E_0 = 70GPa$, and $\nu = 0.3$ and geometrical properties given by $l = 1.0m$, $b = 0.1m$ for two different values beam aspect ratio, $\frac{L}{h} = 5$ and 20 for different axial and transvers material gradation index.

Comparison between the obtained results and those obtained by (Huang and Ouyang 2020) for the maximum normalized deflection, $\bar{W}(x) = \frac{100E_0h^3b}{q_0L^4}w(x)$ at different values of the axial and transverse material gradation index for $L/h = 5$ and 20 for simply supported, SS and clamped- simple, CS beams are illustrated in Table 1. It is observed that an excellent agreement is detected with the corresponding results obtained by (Huang and Ouyang 2020).

On the other hand, comparison between the obtained results and that obtained by(Huang and Ouyang 2020) for the variation of normalized normal stress, $\bar{\sigma}_{xx}(0, z) = \frac{bh}{q_0L}\sigma_{xx}(0, z)$ and the normalized shear stress, $\bar{\tau}_{xz}(\frac{-L}{2}, z) = \frac{bh}{q_0L}\tau_{xz}(\frac{-L}{2}, z)$ with the

normalized beam thickness for $z/h = 5$ are shown in Fig. 3. It may be noticed that the obtained results are in excellent agreement with the corresponding analytical results obtained by (Huang and Ouyang 2020).

4.2 Dynamic behavior

To check the validity of the developed procedure to investigate the vibration behavior of bidirectional functionally graded beams, the dynamic analysis is performed on a beam with reference material properties given by $E_0 = 210GPa$, $\rho_0 = 7850kg/m^3$ and $\mu = 0.3$ and geometrical properties given by $h = 1m$, $b = 0.5m$ and $\frac{L}{h}$ ratio equal to 5 and 20 . The developed numerical procedure is applied to investigate the free as well as the forced vibration behavior under moving load for SS and CS beams. Comparison between the obtained nondimensional frequency parameter, $\lambda_1 = \frac{\omega L^2}{h} \sqrt{\frac{\rho_0}{E_0}}$ and that obtained by (Şimşek 2015) at different material gradation index for $L/h = 5$ for SS and CS bidirectional Timoshenko functionally graded, BDTFG beams are depicted in Table 2. It may be observed that an excellent agreement between the obtained results and the corresponding results obtained by (Şimşek 2015).

To check the forced vibration response of bidirectional functionally graded Timoshenko beams under the moving load, the developed procedure is applied to detect the forced vibration response under moving

Table 2 Dimensionless first natural frequency of SS and CS bidirectional Timoshenko-Ehrenfest functionally graded, BDTEFG beam at $L/h = 5$

BCs	r_z	r_x		0.4		0.6		1.0	
		Şimşek (2015)	Present	Şimşek (2015)	Present	Şimşek (2015)	Present	Şimşek (2015)	Present
SS	0	2.6767	2.6772	2.6728	2.672	2.6650	2.6655	2.6455	2.6448
	0.4	2.6669	2.6677	2.6611	2.6626	2.6552	2.6561	2.6337	2.6355
	0.6	2.6533	2.656	2.6474	2.6509	2.6416	2.6445	2.6201	2.624
	1.0	2.6103	2.6193	2.6044	2.6142	2.5986	2.6079	2.5771	2.5878
CS	0	3.8779	3.8788	3.7685	3.7694	3.7138	3.7142	3.6005	3.6025
	0.4	3.8662	3.867	3.7568	3.758	3.7021	3.703	3.5908	3.5917
	0.6	3.8505	3.8524	3.7431	3.7438	3.6865	3.6891	3.5751	3.5782
	1.0	3.8037	3.8063	3.6962	3.6991	3.6416	3.6451	3.5322	3.5358

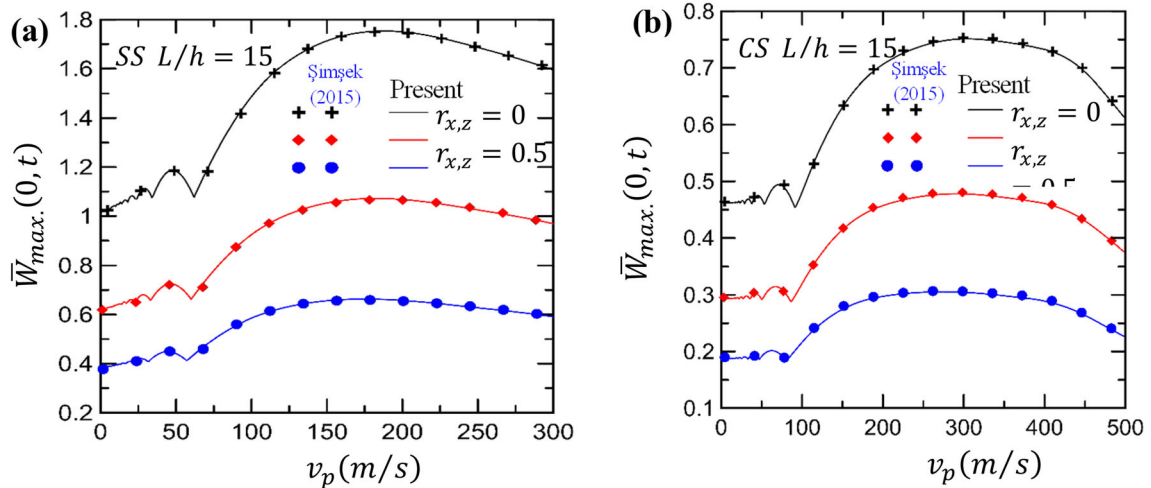


Fig. 4 Variation of the maximum normalized dynamic deflection with the moving load velocity for $\frac{L}{h} = 15$, $v_p = 20m/s$

load and the obtained results for the maximum non-dimensional deflection, $w(0, t) \times \frac{48E_0I}{P_0L^3}$ will be compared with the corresponding results obtained by (Şimşek 2015). Variations of the maximum non-dimensional deflection, $\bar{W}(0, t) = w(0, t) \times \frac{48E_0I}{P_0L^3}$ with the moving load velocity at different material gradation index for both SS and CS beams for $L/h = 15$ are shown in Fig. 4. While the dependency of the maximum non-dimensional deflection, $\bar{W}(0, t)$ on the normalized time, $\bar{t} = \frac{t}{t_f}$ where t_f is the time required for the moving load $v_p = 20m/s$ to reach the end of the beam, at $L/h = 5$ for both SS and CS beams is illustrated in Fig. 5. It is observed that, comparing between the obtained results and those obtained by

(Şimşek 2015), there is an excellent agreement is found validating the developed numerical procedure.

5 Numerical results and discussion

In this section, the static and dynamic behaviors of bidirectional functionally graded beam with different boundary conditions will be studied and analyzed. Symmetrical material distribution through thickness and length based on power-law function will be applied throughout calculations as indicated in Eq. (1a). The reference properties are based on ceramics of alumina with Young's modulus $E_1 = 380GPa$, density $\rho_1 = 3960kg/m^3$ and

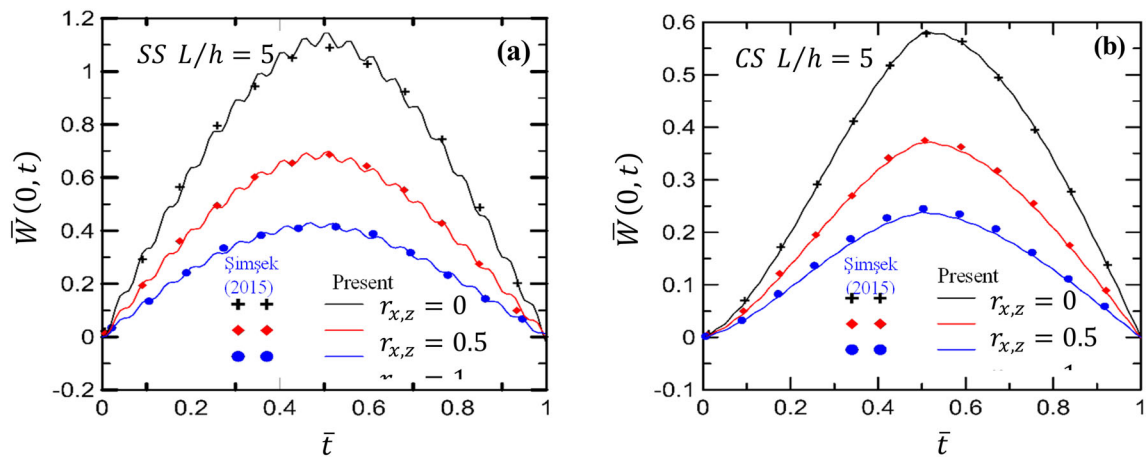


Fig. 5 Time history of the normalized dynamic deflection with the dimensionless time for $L/h = 5$ and $v_p = 20m/s$

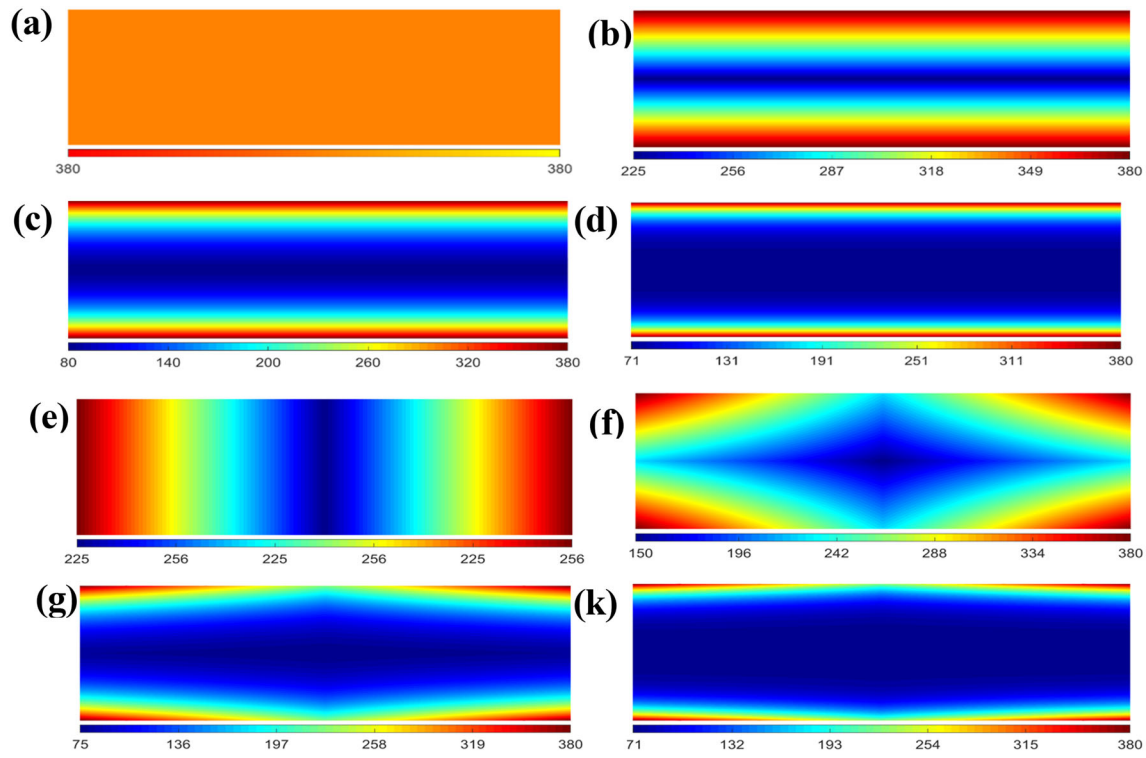


Fig. 6 The distributions of modulus of elasticity through length and thickness ((a) $r_x = 0, r_z = 0$; (b) $r_x = 0, r_z = 1$; (c) $r_x = 0, r_z = 5$; (d) $r_x = 0, r_z = 10$; (e) $r_x = 1, r_z = 0$; (f) $r_x = 1, r_z = 1$; (g) $r_x = 1, r_z = 5$; (k) $r_x = 1, r_z = 10$)

Poisson’s ratio $\mu = 0.3$ and aluminum metal with Young’s modulus $E_2 = 70GPa$, density $\rho_2 = 2700kg/m^3$ and Poisson’s ratio $\mu = 0.3$, Wang and

Zu (2018). Figure 6 shows the effect of graduation index in the variation of properties values is illustrated for young modulus. The geometrical properties

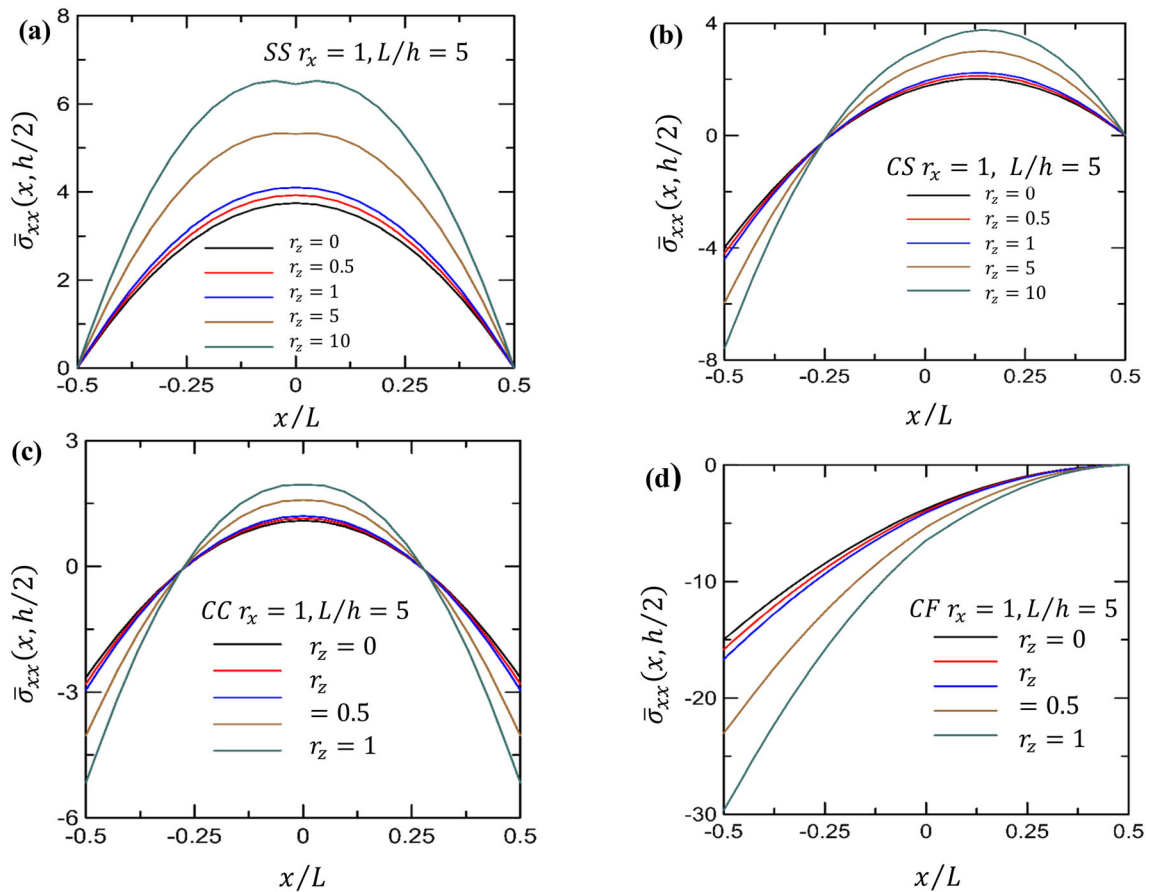


Fig. 7 Dimensionless normal stress through the normalized axial coordinate

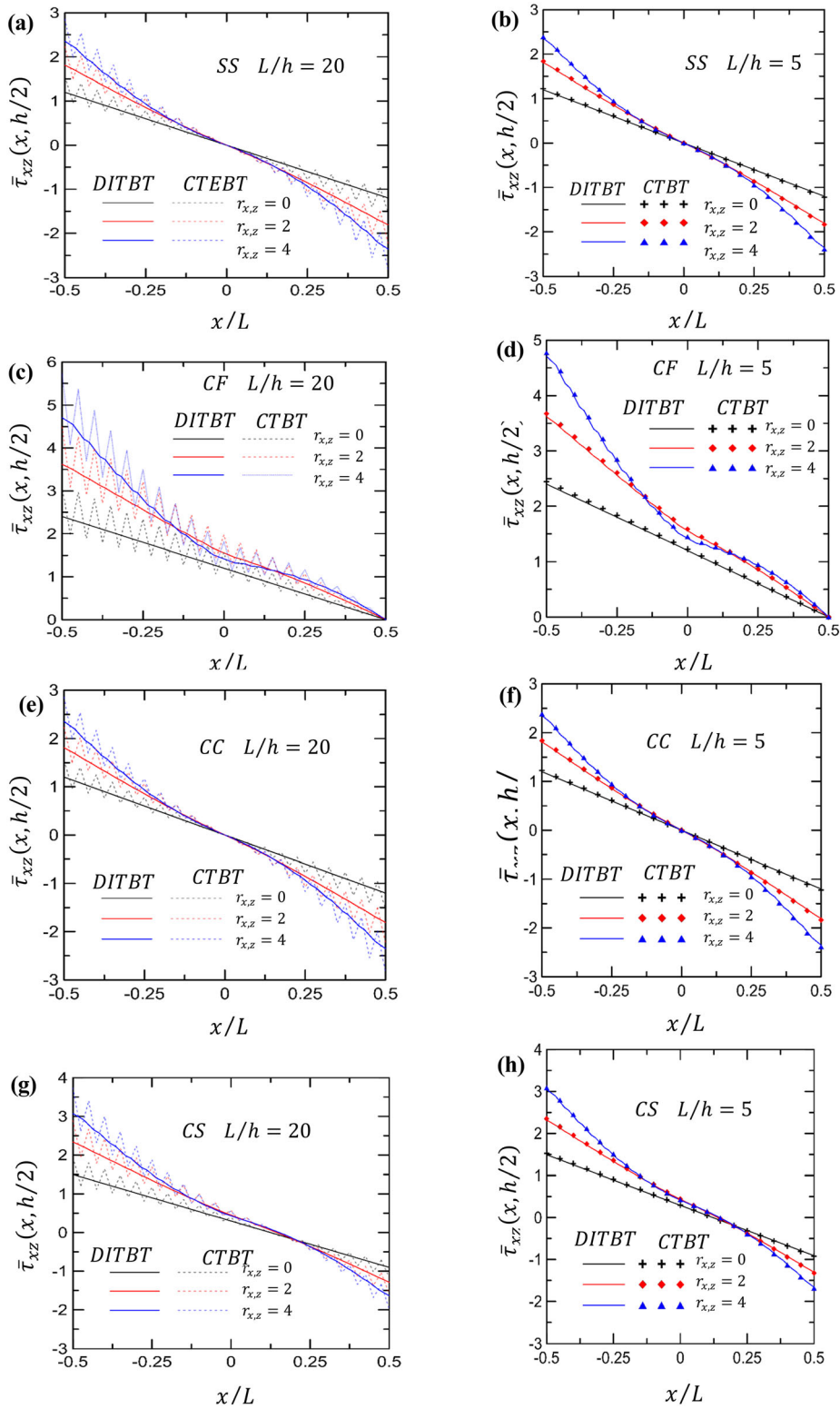
assumed to be $h = 1m$, $b = 0.5m$. To investigate the influence of the boundary conditions on the mechanical behavior of BDTFG beams, four different boundary conditions are considered; Simply supported, SS, Simple-clamped, SC, clamped- clamped CC, and clamped free, CF.

5.1 Static bending behavior

To investigate the static bending behavior of bidirectional functionally graded Timoshenko beam under uniformly distributed load having an intensity of q_0 for different boundary conditions, consider the beam with the geometrical and material characteristics described in Sect. 5. The normalized normal stress at the midplane, $\tilde{\sigma}_{xx}(x, \frac{h}{2}) = \frac{bh}{q_0L} \sigma_{xx}(x, \frac{h}{2})$ profiles throughout the normalized axial coordinate, $\frac{x}{L}$ at axial gradation

index, $r_x = 1$ and beam aspect ratio, $\frac{L}{h} = 5$ for different values of transverse gradation index, r_z at different boundary conditions are illustrated in Fig. 7. It is noticed that increasing the material transverse gradation index increases the material content of metal which increases the overall material flexibility thus increasing the normalized normal stress for all beam boundary conditions. On the other hand, the normalized normal stress significantly affected by the beam boundary condition,; the CF produces the largest values of the maximum normalized normal stress at the midplane while both SS and CC almost produces the same area under the normalized normal stress profile.

To investigate the effectiveness of the developed procedure to efficiently detect the shear stress profile throughout the beam length, the normalized shear



◀ **Fig. 8** Dimensionless shear stress through the normalized axial coordinate for different BCs

stress, $\bar{\tau}_{xz}(x, \frac{h}{2}) = \frac{2bh}{q_0L} \tau_{xz}(x, \frac{h}{2})$ profiles throughout the normalized coordinate, $\frac{x}{L}$ are investigated using 5 noded Timoshenko beam element with different shape function (DITBT) and 3 noded Timoshenko beam element with equal convention shape function (CTBT) for two different values of beam aspect ratio for SS, CF, CC, and CS boundary conditions, as illustrated in Fig. 8. It is observed that both DITBT and CTBT formulations are capable to predict the exact solution in case of thick beam, $\frac{L}{h} = 5$. On the other hand, for slender beam, $\frac{L}{h} = 20$; CTBT indicate inconsistency in shear stress profile due to the disability of convention CTBT to vanish the shear strain to coincide with the exact solution of EBBT and produces oscillatory normalized shear stress profiles due to shear locking phenomena. By using mixed shape function in which the displacement is interpolated with higher order interpolation function than rotation (DITBT), the vanish condition of shear strain is satisfied. As noticed for the normalized normal stress, also the normalized shear stress profiles increase with increasing the material gradation index due to increasing the material content of metal. Moreover, larger values of the maximum normalized shear stress are detected for CF boundary condition comparing with that obtained in SS, CS and CC boundary conditions.

5.2 Free vibration analysis

The developed procedure is applied to solve the eigen value problem to obtain the fundamental frequency of vibrational motion. The influence of the axial and transvers gradation index on the fundamental frequency is detected. Variations of the nondimensional frequency parameter for the first vibration mode, $\lambda_1 = \frac{\omega_1 L^2}{h} \sqrt{\frac{\rho_1}{E_1}}$ with the transverse gradation index, r_z at different values of the axial gradation index, r_x for different beam boundary conditions for BDTFG beam with metallic core are depicted in Fig. 9. It is noticed that, keeping one of the material gradation index constant and increasing the other results in decreasing the first nondimensional natural frequency due to the overall decrease in the system stiffness as well as the

inertia effect with the increase of gradation indices. As it is known from theory of vibration the natural frequency is directly proportional to the modulus of elasticity and inversely proportional to the mass density that is why for the first moment it could be thought that the modulus elasticity has the dominated effect in natural frequency but this is not clear yet as for the given material ingredients the elasticity can change from minimum value $70GPa$ to maximum value $380GPa$ with 5.4 times increasing ratio while density can change from minimum value $2700Kg/m^3$ to maximum value of $3960Kg/m^3$ with 1.46 times increasing ratio which tend to be constant density compared to the change in elasticity and that is mean the effect of density variation is not cleared for the given material ingredients. In these results the change in natural frequency is tend to obey the change in density by decreasing with the increasing of density otherwise increasing with the increasing of elasticity which mean for the same changing ratio for elasticity and density; the density will has the dominated effect in natural frequency.

Reversing the material distribution such that beam core is almost ceramic, dependency of the first nondimensional natural frequency on the material gradation indices for different beam boundary conditions for ($L/h = 5$) beams are illustrated in Table 3. It is observed that, keeping constant value of one of the material gradation index, increasing the material gradation index in either transverse or axial direction increases the material content of ceramic leading to higher values of stiffness and consequently higher values of natural frequencies are observed. Moreover, at higher values of the material gradation index in either axial or transverse direction, (r_x or $r_z = 10$) almost constant nondimensional frequency parameter is detected. Comparing between the boundary conditions, CF beams produces the smallest nondimensional natural frequencies while the largest nondimensional natural frequencies are detected for CC beams. Additionally, beam aspect ratio significantly affect the detected natural frequency. Higher values of natural frequency are detected with increasing beam aspect ratio.

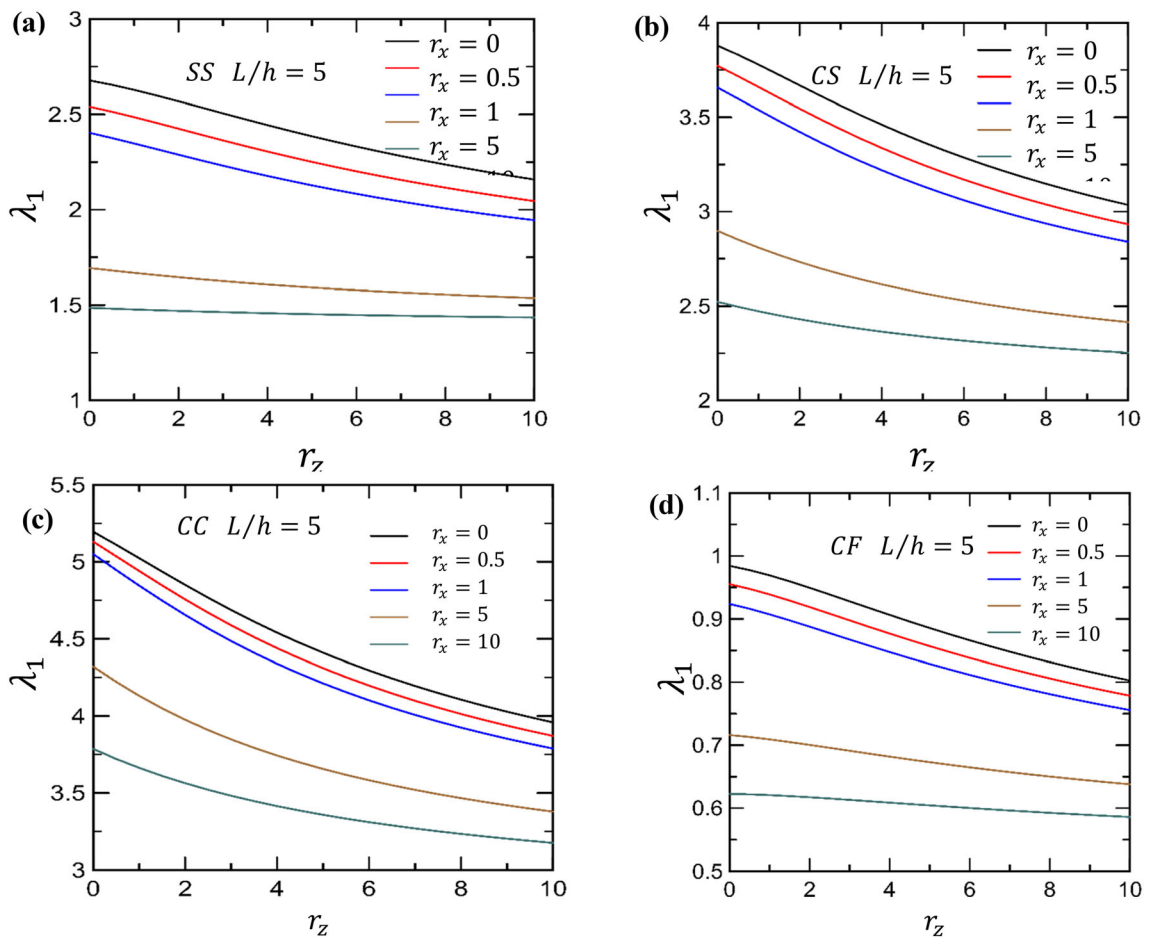


Fig. 9 The non-dimensional first natural frequency versus r_z for $L/h = 5$, for BDTEFG beams with almost metallic core

Table 3 Dimensionless first natural frequency of bidirectional Timoshenko-Ehrenfest functionally graded BDTEFG beam with ceramic core for SS, CS, CC, and CF boundary conditions at $L/h = 5$

r_z	The nondimensional natural frequency λ_1									
	r_x					r_x				
	0	0.5	1	5	10	0	0.5	1	5	10
	SS					CS				
0	1.3916	1.7702	1.9747	2.474	2.5925	2.0162	2.3912	2.5963	3.164	3.3916
0.5	1.5478	1.867	2.0498	2.5053	2.6085	2.2712	2.5801	2.7596	3.2631	3.4575
1	1.6619	1.9380	2.1034	2.5252	2.6188	2.4492	2.7135	2.8740	3.3331	3.5059
5	2.0954	2.2299	2.3234	2.5909	2.6489	3.0897	3.2146	3.3029	3.5830	3.6815
10	2.2980	2.3799	2.4398	2.6201	2.6595	3.3726	3.4476	3.5035	3.6899	3.7547
	CC					CF				
0	2.7001	3.0610	3.2586	3.8757	4.2140	0.5116	0.5867	0.6293	0.7727	0.8474
0.5	3.0789	3.3674	3.5336	4.0575	4.3415	0.5665	0.6287	0.6665	0.7962	0.8621
1	3.3346	3.5778	3.7237	4.1885	4.4369	0.6073	0.6609	0.6950	0.8142	0.8737
5	4.2083	4.3192	4.3966	4.6613	4.7925	0.7654	0.7916	0.8110	0.8854	0.9205
10	4.5726	4.6380	4.6864	4.8590	4.9422	0.8408	0.8569	0.8694	0.9195	0.9429

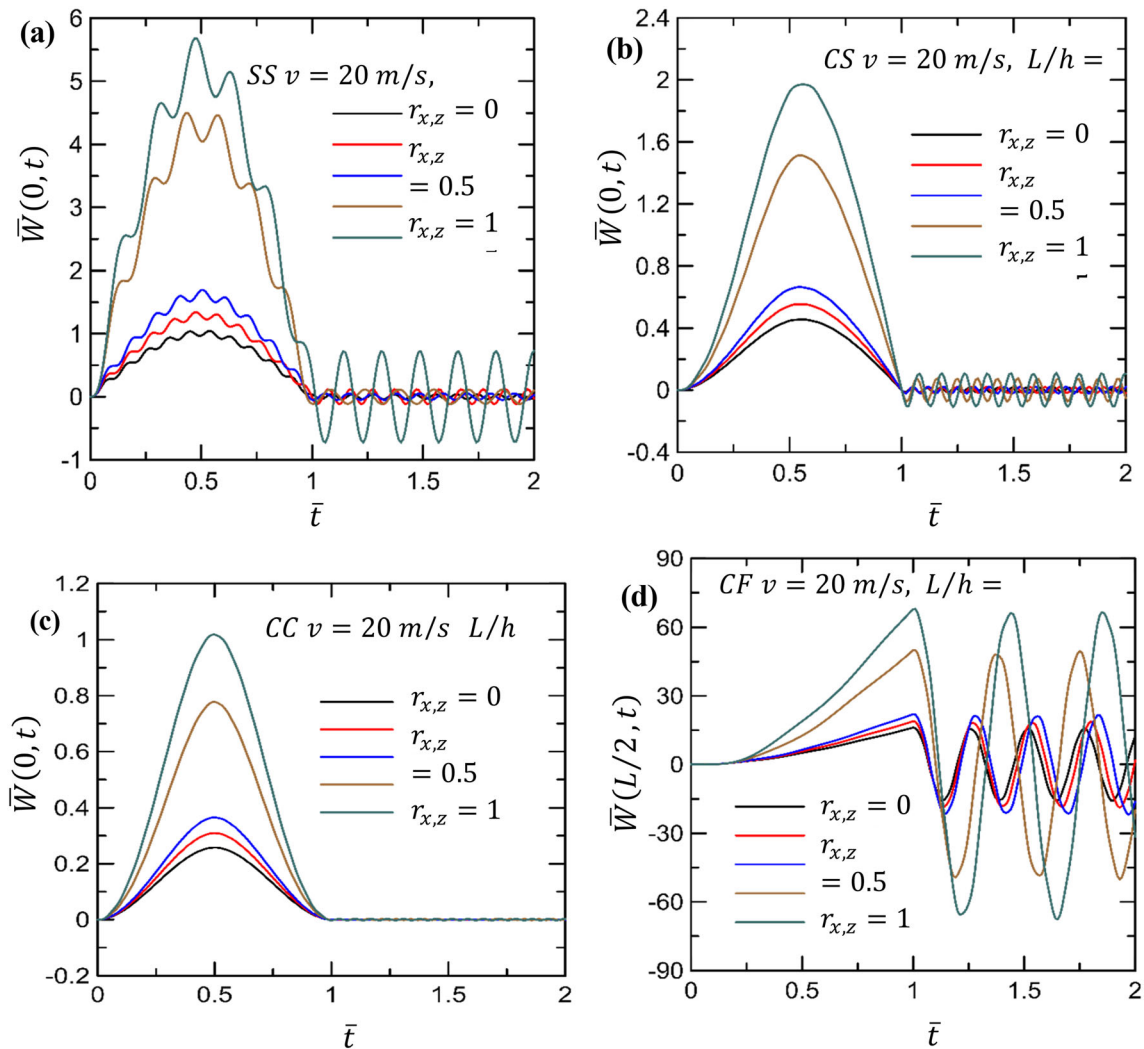


Fig. 10 Time history of the normalized dynamic deflection with the dimensionless time for $\frac{L}{h} = 20$ and $v_p = 20\text{m/s}$ for BDTFG beams with metallic core

5.3 Forced vibration response under moving load

The forced vibration time response under moving point load of intensity of P_0 , is investigated for material gradation indices and different beam boundary conditions. The load velocity is set to be equal $v_p = 20\text{m/s}$ and the aspect ratio, L/h equal 20. The normalized central deflection, $\bar{W}(0, t) = w(0, t) \times \frac{48E_1I}{P_0L^3}$ profiles for SS, CS and CC and The normalized free end deflection, $\bar{W}(L/2, t) = w(L/2, t) \times \frac{48E_1I}{P_0L^3}$ profiles for CF versus the normalized time, $\bar{t} = \frac{t v_p}{L}$ for different values of material gradation index are depicted in Fig. 10. It is observed that the material

gradation indices significantly affect the forced vibration response under moving load; increasing the material gradation index in axial and transverse directions increases the transverse deflection for all beam boundary conditions due to decreasing the overall system stiffness which increases the system flexibility.

Additionally, the boundary condition significantly affects both value and smoothness of the nondimensional transverse deflection with time. CC beam behaves quasi-statically under the action moving load, ($0 \leq \bar{t} \leq 1$) and after removing the action of load ($\bar{t} > 1$). On the other hand both CS and CF behave quasi-statically throughout the time interval of load

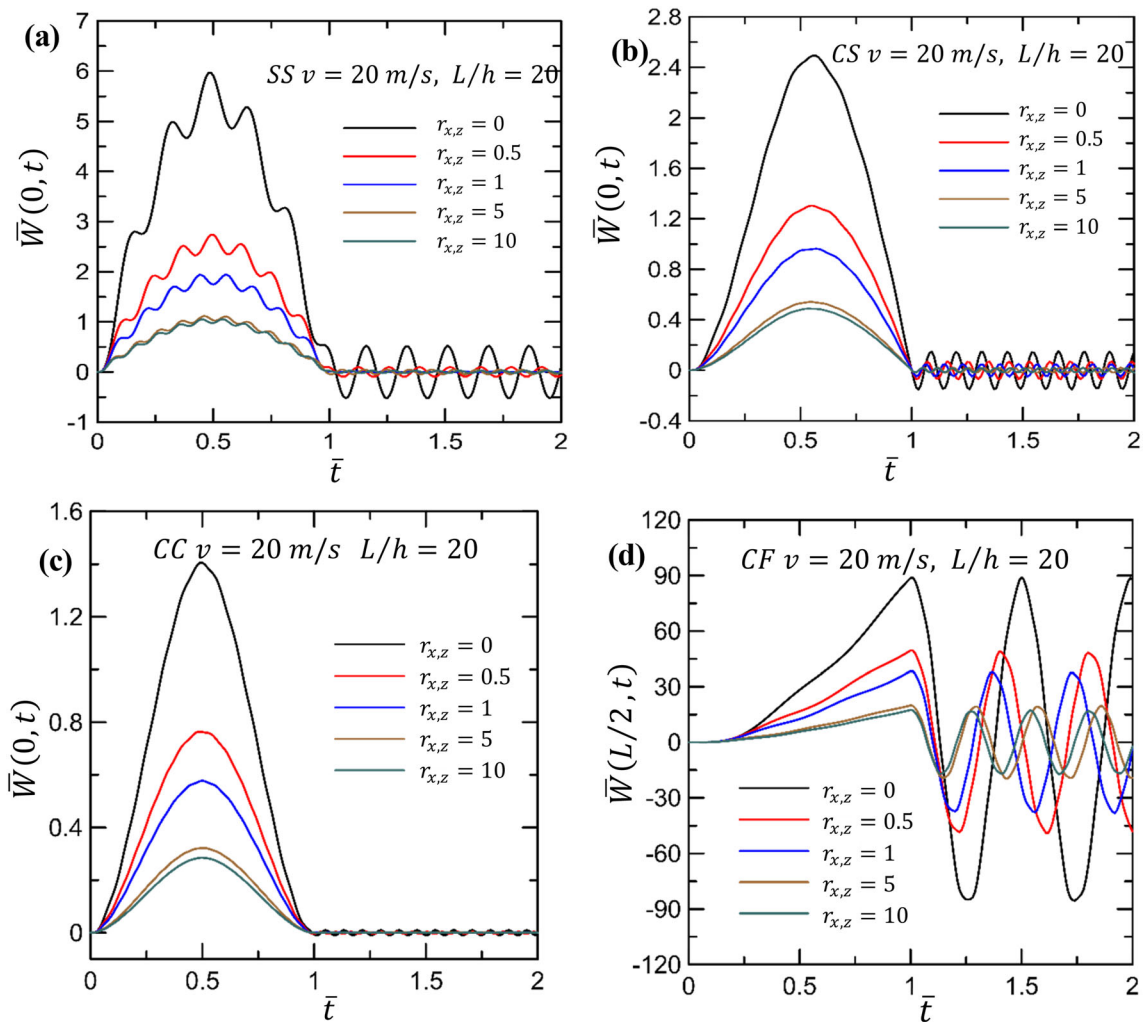


Fig. 11 Time history of the normalized dynamic deflection with the dimensionless time for $\frac{L}{h} = 20$ and $v_p = 20$ m/s for different BCs. for BDTFG beams with ceramic core

application, ($0 \leq \bar{t} \leq 1$) while oscillating waves are associated with the transverse deflection profile after load leaving the beam span, ($\bar{t} > 1$). On contrary to the CC, SS beam produces a normalized transverse bending profiles associated with oscillating wave during the intervals of application and removal of load. Moreover, the maximum normalized deflection is detected for CF beam while the smallest value is produced by the CC beam.

On the other hand this trend is reversed if the material properties are distributed such that beam core is fully ceramic. As shown in Fig. 11, the maximum normalized transverse deflection under moving load

decreases with increasing the material gradation index.

It is observed that the effect of increasing the moving load velocity is controlled by the material gradation indices, the beam aspect ratio and the beam boundary conditions. Depending on the beam aspect ratio and the boundary conditions, increasing the moving load velocity below the critical speed produces either constant transverse deflection profile or slow rate increasing one. On the other hand, for thin beams, $L/h = 20$, as the speed increases over the critical value the transverse deflection increases until reaching maximum value then decreases or proceeds

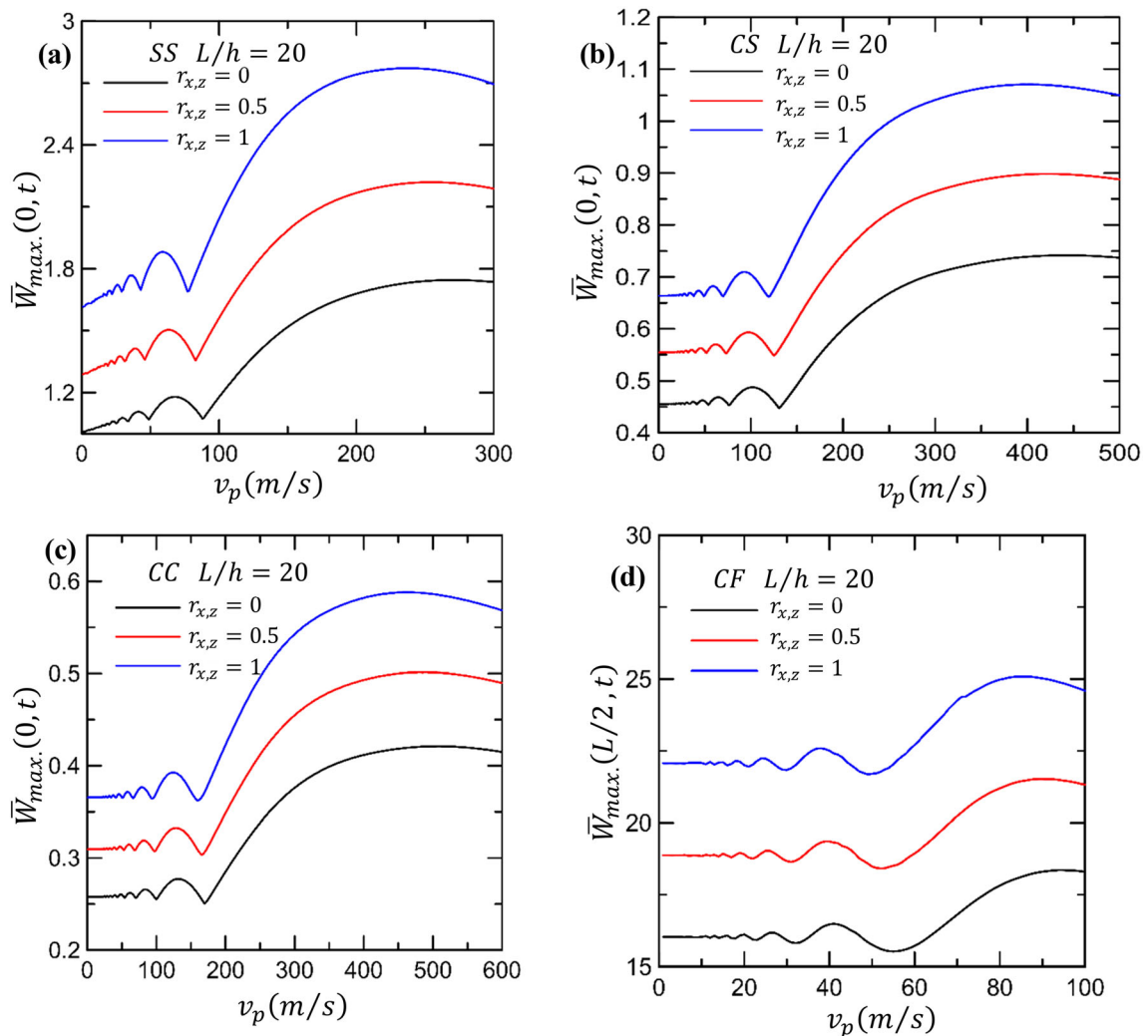


Fig. 12 Variation of the maximum normalized dynamic deflection with the load velocity for $L/h = 20$, for different BCs

with a constant value depending on the material gradation indices and boundary conditions. Moreover, for CF thick beams, the moving load velocity has insignificant effect on the maximum transverse deflection. Thin beams behave quasi-statically as the moving load speed increases above its critical value while transverse deflection profile associated with oscillating waves is detected for thick beams. The amplitudes of the associated waves depend on the beam boundary conditions; waves with increasing amplitudes are observed for SS, CS, and CC while it is completely disappeared for CF thick beams.

The speed of the applied moving load significantly the maximum transverse deflection. Variations of the normalized maximum transverse deflection, deflection $\bar{W}_{max.}(x, t) = w(x, t) \times \frac{48E_1L}{P_0L^3}$, evaluated at the mid beam ($x = 0$) for SS, CS and CC and at the free end of the beam ($x = L/2$) for CF beam, with the applied moving load speed for different material gradation index in the axial and transverse directions for both thin and thick beams are respectively illustrated in Figs. 12 and 13.

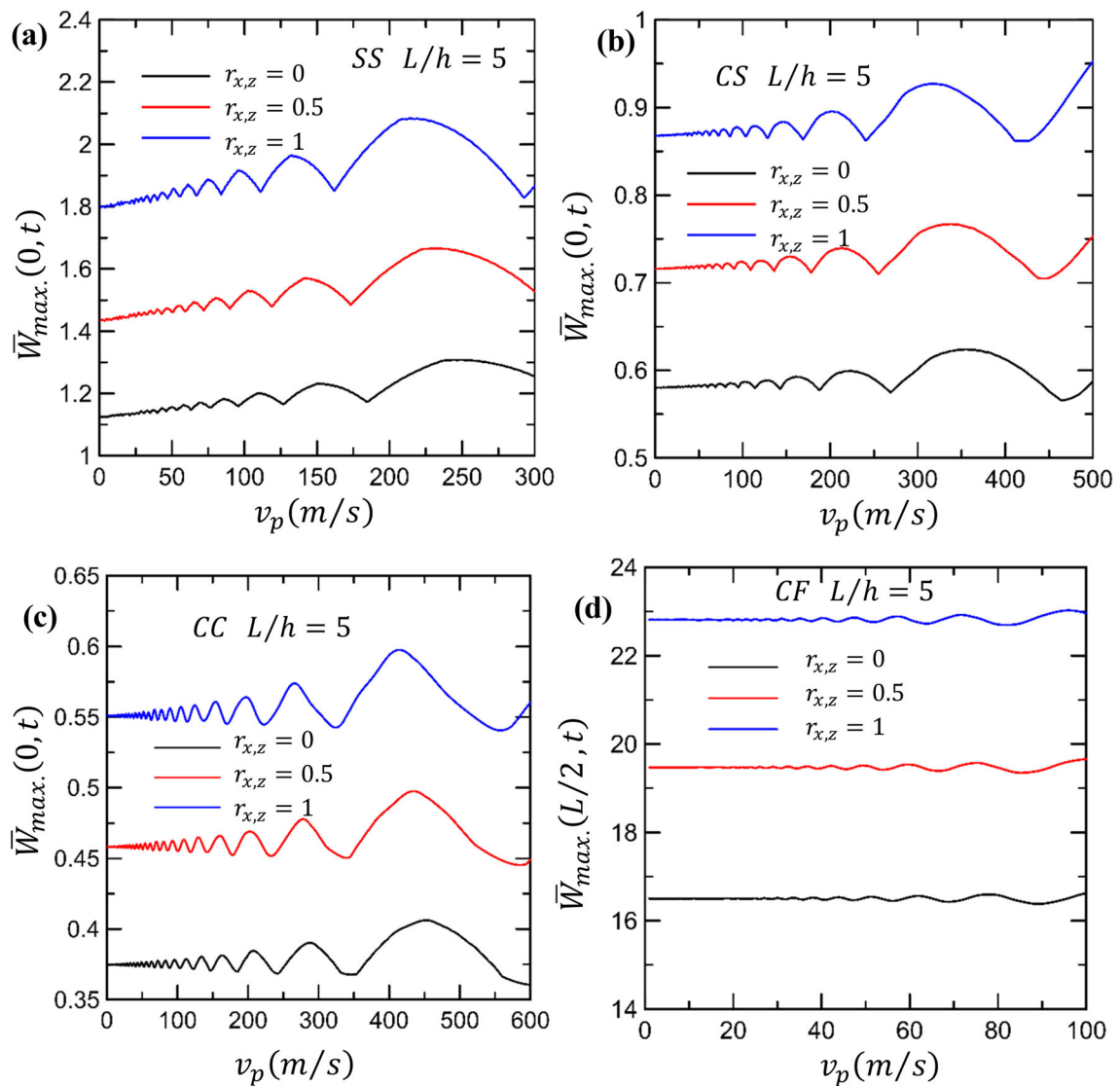


Fig. 13 Variation of the maximum normalized dynamic deflection with moving load velocity for $L/h = 5$ for different BCs

6 Conclusions

Static and dynamic mechanical behaviors of bidirectional symmetrical functionally graded Timoshenko beams considering the shear locking effect is investigated through finite element procedure. Different polynomial shape functions are used to avoid shear locking phenomena occurs in thin beams. The material properties of the functionally graded materials are assumed to be graduated through both axial and transverse directions according to the power law

function. To maintain the outer fibers of the beam against rubbing conditions or strengthen beam core, symmetrical material properties distribution is assumed such that both upper and bottom surface are harder than beam core or core be harder than top and bottom beam fibers. The differential equations of motion are derived using the virtual displacement principle. To avoid shear locking, the dynamic finite element equations of motion are derived on mixed shape function basis. The incremental solution procedure based on implicit direct integration technique is

presented. The developed numerical methodology is verified for static and dynamic analysis and good agreement is observed. Numerical results are obtained and discussed. Based on the considered material and geometrical parameters, the following concluding remarks are revealed:

- The material gradation index in the axial and transverse direction significantly affect the mechanical behavior of bidirectional symmetrical functionally graded materials; increasing the material gradation index increases the flexibility of beam and consequently larger values of the transverse deflection and the produced stresses are detected while smaller values of the natural frequencies are observed.
- To seek efficient detection of the mechanical behavior of Timoshenko beams, finite elements based on mixed shape functions could be used to avoid shear locking phenomena occurs in thin beam structures.
- The mechanical behavior of bidirectional symmetrical functionally graded Timoshenko beam under moving load significantly affected by the beam boundary conditions. For thin beams, $L/h = 20$, CC beam produces a more stable dynamic behavior under moving load compared with SS, CF, CS beams.
- The applied moving load speed has a significant effect on the forced vibration response, this effect is controlled with the material gradation index, beam aspect ratio, and the beam boundary conditions.
- Beam aspect ratio significantly affects the forced time response. This ratio should be carefully chosen to attain stable dynamic performance.
- Symmetrical material gradation could be used for enhancing the mechanical performance of beam structural components according to the required objective.

References

Abdelrahman, A.A., El-Shafei, A.G.: Modeling and analysis of the transient response of viscoelastic solids. *Waves Random Complex Media* (2020). <https://doi.org/10.1080/17455030.2020.1714790>

- Abdelrahman, A.A., Eltaher, M.A.: On bending and buckling responses of perforated nanobeams including surface energy for different beams theories. *Eng. Comput.* (2020). <https://doi.org/10.1007/s00366-020-01211-8>
- Akbaş, Ş.D., Fageehi, Y.A., Assie, A.E., Eltaher, M.A.: Dynamic analysis of viscoelastic functionally graded porous thick beams under pulse load. *Eng. Comput.* (2020). <https://doi.org/10.1007/s00366-020-01070-3>
- Alshorbagy, A.E., Eltaher, M.A., Mahmoud, F.F.: Free vibration characteristics of a functionally graded beam by finite element method. *Appl. Math. Model.* **35**(1), 412–425 (2011). <https://doi.org/10.1016/j.apm.2010.07.006>
- Atmane, H.A., Tounsi, A., Bernard, F.: Effect of thickness stretching and porosity on mechanical response of a functionally graded beams resting on elastic foundations. *Int. J. Mech. Mater. Des.* **13**(1), 71–84 (2017). <https://doi.org/10.1007/s10999-015-9318-x>
- Attia, M.A., Mohamed, S.A.: Nonlinear thermal buckling and postbuckling analysis of bidirectional functionally graded tapered microbeams based on Reddy beam theory. *Eng. Comput.* (2020). <https://doi.org/10.1007/s00366-020-01080-1>
- Attia, M.A., Abdelrahman, A.A.: On vibrations of functionally graded viscoelastic nanobeams with surface effects. *Int. J. Eng. Sci.* **127**, 1–32 (2018). <https://doi.org/10.1016/j.ijengsci.2018.02.005>
- Baier-Saip, J.A., Baier, P.A., de Faria, A.R., Oliveira, J.C., Baier, H.: Shear locking in one-dimensional finite element methods. *Eur. J. Mech. a. Solids* **79**, 103871 (2020). <https://doi.org/10.1016/j.euromechsol.2019.103871>
- Borst, R., Crisfield, M., Remmers, J., Verhoosel, C.: Non-linear finite element analysis of solids and structures, 2nd edn. Wiley, Chichester (2012). <https://doi.org/10.1002/9781118375938>
- Bouazza, M., Zenkour, A.M.: Hygro-thermo-mechanical buckling of laminated beam using hyperbolic refined shear deformation theory. *Compos. Struct.* **252**, 112689 (2020). <https://doi.org/10.1016/j.compstruct.2020.112689>
- Boussoula, A., Boucham, B., Bourada, M., Bourada, F., Tounsi, A., Bousahla, A.A., Tounsi, A.: A simple nth-order shear deformation theory for thermomechanical bending analysis of different configurations of FG sandwich plates. *Smart Struct. Syst.* **25**(2), 197–218 (2020). <https://doi.org/10.12989/SSS.2020.25.2.197>
- Carrera, E.: Theories and finite elements for multilayered plates and shells: a unified compact formulation with numerical assessment and benchmarking. *Arch. Comput. Methods Eng.* **10**(3), 215–296 (2003)
- Deng, H., Cheng, W.: Dynamic characteristics analysis of bi-directional functionally graded Timoshenko beams. *Compos. Struct.* **141**, 253–263 (2016). <https://doi.org/10.1016/j.compstruct.2016.01.051>
- Ebrahimi-Mamaghani, A., Sarparast, H., Rezaei, M.: On the vibrations of axially graded Rayleigh beams under a moving load. *Appl. Math. Model.* **84**, 554–570 (2020). <https://doi.org/10.1016/j.apm.2020.04.002>
- Edem, I.B.: The exact two-node Timoshenko beam finite element using analytical bending and shear rotation interdependent shape functions. *Int. J. Comput. Methods Eng. Sci. Mech.* **7**(6), 425–431 (2006). <https://doi.org/10.1080/15502280600826381>

- Elishakoff, I.E.: Handbook on Timoshenko-Ehrenfest beam and Uflyand-Mindlin plate theories. World Scientific, Singapore (2019)
- Elishakoff, I.E.: Who developed the so-called Timoshenko beam theory? *Math. Mech. Solids* **25**(1), 97–116 (2020). <https://doi.org/10.1177/1081286519856931>
- Elishakoff, I.E., Pentaras, D., Gentilini, C.: *Mechanics of functionally graded material structures*. World Scientific/Imperial College Press, Singapore (2015)
- Eltaher, M.A., Abdelrahman, A.A., Al-Nabawy, A., Khater, M., Mansour, A.: Vibration of nonlinear graduation of nano-Timoshenko beam considering the neutral axis position. *Appl. Math. Comput.* **235**, 512–529 (2014). <https://doi.org/10.1016/j.amc.2014.03.028>
- Eltaher, M.A., Alshorbagy, A.E., Mahmoud, F.F.: Determination of neutral axis position and its effect on natural frequencies of functionally graded macro/nanobeams. *Compos. Struct.* **99**, 193–201 (2013). <https://doi.org/10.1016/j.compstruct.2012.11.039>
- Esen, I.: Dynamic response of a functionally graded Timoshenko beam on two -parameter elastic foundations due to a variable velocity moving mass. *Int. J. Mech. Sci.* **153**, 21–35 (2019a). <https://doi.org/10.1016/j.ijmecsci.2019.01.033>
- Esen, I.: Dynamic response of functional graded Timoshenko beams in a thermal environment subjected to an accelerating load. *Eur. J. Mech. A/solids* **78**, 103841 (2019b). <https://doi.org/10.1016/j.euromechsol.2019.103841>
- Esen, I.: Dynamics of size-dependant Timoshenko micro beams subjected to moving loads. *Int. J. Mech. Sci.* **175**, 105501 (2020a). <https://doi.org/10.1016/j.ijmecsci.2020.105501>
- Esen, I.: Response of a micro-capillary system exposed to a moving mass in magnetic field using nonlocal strain gradient theory. *Int. J. Mech. Sci.* **188**, 105937 (2020b). <https://doi.org/10.1016/j.ijmecsci.2020.105937>
- Esen, I., Koc, M.A., Cay, Y.: Finite element formulation and analysis of a functionally graded Timoshenko beam subjected to an accelerating mass including inertial effects of the mass. *Lat. Am. J. Solids Struct.* (2018). <https://doi.org/10.1590/1679-78255102>
- Esen, I., Özarpa, C., Eltaher, M.A.: Free vibration of a cracked FG microbeam embedded in an elastic matrix and exposed to magnetic field in a thermal environment. *Compos. Struct.* **261**, 113552 (2021). <https://doi.org/10.1016/j.apm.2021.03.008>
- Ghatage, P.S., Kar, V.R., Sudhagar, P.E.: On the numerical modelling and analysis of multi-directional functionally graded composite structures: a review. *Compos. Struct.* **236**, 111837 (2020). <https://doi.org/10.1016/j.compstruct.2019.111837>
- Hu, H., Yu, T., Lich, L.V., Bui, T.Q.: Functionally graded curved Timoshenko microbeams: a numerical study using IGA and modified couple stress theory. *Compos. Struct.* **254**, 112841 (2020). <https://doi.org/10.1016/j.compstruct.2020.112841>
- Huang, Y.: Bending and free vibrational analysis of bi-directional functionally graded beams with circular cross-section. *Appl. Math. Mech.* **41**(10), 1497–1516 (2020). <https://doi.org/10.1007/s10483-020-2670-6>
- Huang, Y., Li, X.-F.: A new approach for free vibration of axially functionally graded beams with non-uniform cross-section. *J. Sound Vib.* **329**(11), 2291–2303 (2010). <https://doi.org/10.1016/j.jsv.2009.12.029>
- Huang, Y., Ouyang, Z.-Y.: Exact solution for bending analysis of two-directional functionally graded Timoshenko beams. *Arch. Appl. Mech.* **90**(5), 1005–1023 (2020). <https://doi.org/10.1007/s00419-019-01655-5>
- Huang, Y., Yang, L.-E., Luo, Q.-Z.: Free vibration of axially functionally graded Timoshenko beams with non-uniform cross-section. *Compos. B Eng.* **45**(1), 1493–1498 (2013). <https://doi.org/10.1016/j.compositesb.2012.09.015>
- Jamshidi, M., Arghavani, J., Maboudi, G.: Post-buckling optimization of two-dimensional functionally graded porous beams. *Int. J. Mech. Mater. Des.* **15**(4), 801–815 (2019). <https://doi.org/10.1007/s10999-019-09443-3>
- Jha, D.K., Kant, T., Singh, R.K.: A critical review of recent research on functionally graded plates. *Compos. Struct.* **96**, 833–849 (2013). <https://doi.org/10.1016/j.compstruct.2012.09.001>
- Jiang, Z.-C., Ma, W.-L., Li, X.-F.: Stability of cantilever on elastic foundation under a subtangential follower force via shear deformation beam theories. *Thin-Walled Struct.* **154**, 106853 (2020). <https://doi.org/10.1016/j.tws.2020.106853>
- Jing, L.-L., Ming, P.-J., Zhang, W.-P., Fu, L.-R., Cao, Y.-P.: Static and free vibration analysis of functionally graded beams by combination Timoshenko theory and finite volume method. *Compos. Struct.* **138**, 192–213 (2016). <https://doi.org/10.1016/j.compstruct.2015.11.027>
- Kadoli, R., Akhtar, K., Ganesan, N.: Static analysis of functionally graded beams using higher order shear deformation theory. *Appl. Math. Model.* **32**(12), 2509–2525 (2008). <https://doi.org/10.1016/j.apm.2007.09.015>
- Karama, M., Afaq, K.S., Mistou, S.: Mechanical behaviour of laminated composite beam by the new multi-layered laminated composite structures model with transverse shear stress continuity. *Int. J. Solids Struct.* **40**(6), 1525–1546 (2003). [https://doi.org/10.1016/S0020-7683\(02\)00647-9](https://doi.org/10.1016/S0020-7683(02)00647-9)
- Karamanli, A.: Elastostatic analysis of two-directional functionally graded beams using various beam theories and symmetric smoothed particle hydrodynamics method. *Compos. Struct.* **160**, 653–669 (2017). <https://doi.org/10.1016/j.compstruct.2016.10.065>
- Karamanli, A.: Free vibration analysis of two directional functionally graded beams using a third order shear deformation theory. *Compos. Struct.* **189**, 127–136 (2018). <https://doi.org/10.1016/j.compstruct.2018.01.060>
- Khoshgoftar, M.J.: Second order shear deformation theory for functionally graded axisymmetric thick shell with variable thickness under non-uniform pressure. *Thin-Walled Struct.* **144**, 106286 (2019). <https://doi.org/10.1016/j.tws.2019.106286>
- Kieback, B., Neubrand, A., Riedel, H.: Processing techniques for functionally graded materials. *Mater. Sci. Eng. A* **362**(1), 81–106 (2003). [https://doi.org/10.1016/S0921-5093\(03\)00578-1](https://doi.org/10.1016/S0921-5093(03)00578-1)
- Le, C.I., Le, N.A.T., Nguyen, D.K.: Free vibration and buckling of bidirectional functionally graded sandwich beams using an enriched third-order shear deformation beam element. *Compos. Struct.* (2020). <https://doi.org/10.1016/j.compstruct.2020.113309>
- Lee, J.W., Lee, J.Y.: Free vibration analysis of functionally graded Bernoulli-Euler beams using an exact transfer

- matrix expression. *Int. J. Mech. Sci.* **122**, 1–17 (2017). <https://doi.org/10.1016/j.ijmecsci.2017.01.011>
- Li, S.R., Batra, R.C.: Relations between buckling loads of functionally graded Timoshenko and homogeneous Euler-Bernoulli beams. *Compos. Struct.* **95**, 5–9 (2013). <https://doi.org/10.1016/j.compstruct.2012.07.027>
- Liew, K.M., Lei, Z.X., Zhang, L.W.: Mechanical analysis of functionally graded carbon nanotube reinforced composites: a review. *Compos. Struct.* **120**, 90–97 (2015). <https://doi.org/10.1016/j.compstruct.2014.09.041>
- Liu, N., Jeffers, A.E.: Isogeometric analysis of laminated composite and functionally graded sandwich plates based on a layerwise displacement theory. *Compos. Struct.* **176**, 143–153 (2017). <https://doi.org/10.1016/j.compstruct.2017.05.037>
- Liu, N., Jeffers, A.E.: A geometrically exact isogeometric Kirchhoff plate: feature-preserving automatic meshing and C 1 rational triangular Bézier spline discretizations. *Int. J. Numer. Meth. Eng.* **115**(3), 395–409 (2018). <https://doi.org/10.1002/nme.5809>
- Liu, N., Ren, X., Lua, J.: An isogeometric continuum shell element for modeling the nonlinear response of functionally graded material structures. *Compos. Struct.* **237**, 111893 (2020). <https://doi.org/10.1016/j.compstruct.2020.111893>
- Lu, Y., Chen, X.: Nonlinear parametric dynamics of bidirectional functionally graded beams. *Shock. Vib.* **2020**, 8840833 (2020). <https://doi.org/10.1155/2020/8840833>
- Maia, C.D.C.D., Brito, W.K.F., Mendonca, A.V.: A static boundary element solution for Bickford-Reddy beam. *Eng. Comput.* **36**(4), 1435–1451 (2020). <https://doi.org/10.1007/s00366-019-00774-5>
- Malekzadeh, P., Heydarpour, Y.: Free vibration analysis of rotating functionally graded cylindrical shells in thermal environment. *Compos. Struct.* **94**(9), 2971–2981 (2012). <https://doi.org/10.1016/j.compstruct.2012.04.011>
- Menaai, R., Tounsi, A., Mouaici, F., Mechab, I., Zidi, M., Bedia, E.A.A.: Analytical solutions for static shear correction factor of functionally graded rectangular beams. *Mech. Adv. Mater. Struct.* **19**(8), 641–652 (2012). <https://doi.org/10.1080/15376494.2011.581409>
- Mohammadian, M.: Nonlinear free vibration of damped and undamped bi-directional functionally graded beams using a cubic-quintic nonlinear model. *Compos. Struct.* **255**, 112866 (2021). <https://doi.org/10.1016/j.compstruct.2020.112866>
- Mukherjee, S., Prathap, G.: Analysis of shear locking in Timoshenko beam elements using the function space approach. *Commun. Numer. Methods Eng.* **17**(6), 385–393 (2001). <https://doi.org/10.1002/cnm.413>
- Naebe, M., Shirvanimoghaddam, K.: Functionally graded materials: a review of fabrication and properties. *Appl. Mater. Today* **5**, 223–245 (2016). <https://doi.org/10.1016/j.apmt.2016.10.001>
- Nguyen, D.K., Nguyen, Q.H., Tran, T.T., Bui, V.T.: Vibration of bi-dimensional functionally graded Timoshenko beams excited by a moving load. *Acta Mech.* **228**(1), 141–155 (2017). <https://doi.org/10.1007/s00707-016-1705-3>
- Nguyen, D.K., Vu, A.N.T., Le, N.A.T., Pham, V.N.: Dynamic behavior of a bidirectional functionally graded sandwich beam under nonuniform motion of a moving load. *Shock. Vib.* **2020**, 8854076 (2020a). <https://doi.org/10.1155/2020/8854076>
- Nguyen, Q.H., Nguyen, L.B., Nguyen, H.B., Nguyen-Xuan, H.: A three-variable high order shear deformation theory for isogeometric free vibration, buckling and instability analysis of FG porous plates reinforced by graphene platelets. *Compos. Struct.* **245**, 112321 (2020b). <https://doi.org/10.1016/j.compstruct.2020.112321>
- Nguyen, T.-K., Vo, T.P., Thai, H.-T.: Static and free vibration of axially loaded functionally graded beams based on the first-order shear deformation theory. *Compos. B Eng.* **55**, 147–157 (2013). <https://doi.org/10.1016/j.compositesb.2013.06.011>
- Nie, G., Zhong, Z.: Dynamic analysis of multi-directional functionally graded annular plates. *Appl. Math. Model.* **34**(3), 608–616 (2010). <https://doi.org/10.1016/j.apm.2009.06.009>
- Nikbakht, S., Kamarian, S., Shakeri, M.: A review on optimization of composite structures Part II: functionally graded materials. *Compos. Struct.* **214**, 83–102 (2019). <https://doi.org/10.1016/j.compstruct.2019.01.105>
- Oñate, E.: *Structural analysis with the finite element method. Linear statics: beams plates and shells, vol. 2.* Springer, Dordrecht (2013)
- Özarpa, C., Esen, I.: Modelling the dynamics of a nanocapillary system with a moving mass using the non-local strain gradient theory. *Math. Methods Appl. Sci.* (2020). <https://doi.org/10.1002/mma.6812>
- Özarpa, C., Esen, I.: Modelling the dynamics of a nanocapillary system with a moving mass using the non-local strain gradient theory. *Math. Methods Appl. Sci.* (2020). <https://doi.org/10.1002/mma.6812>
- Pradhan, K.K., Chakraverty, S.: Generalized power-law exponent based shear deformation theory for free vibration of functionally graded beams. *Appl. Math. Comput.* **268**, 1240–1258 (2015). <https://doi.org/10.1016/j.amc.2015.07.032>
- Pydah, A., Sabale, A.: Static analysis of bi-directional functionally graded curved beams. *Compos. Struct.* **160**, 867–876 (2017). <https://doi.org/10.1016/j.compstruct.2016.10.120>
- Qin, B., Zhong, R., Wang, Q., Zhao, X.: A Jacobi-Ritz approach for FGP beams with arbitrary boundary conditions based on a higher-order shear deformation theory. *Compos. Struct.* **247**, 112435 (2020). <https://doi.org/10.1016/j.compstruct.2020.112435>
- Reddy, J.N.: A simple higher-order theory for laminated composite plates. *J. Appl. Mech.* **51**(4), 745–752 (1984). <https://doi.org/10.1115/1.3167719>
- Reddy, J.N.: On locking-free shear deformable beam finite elements. *Comput. Methods Appl. Mech. Eng.* **149**(1), 113–132 (1997). [https://doi.org/10.1016/S0045-7825\(97\)00075-3](https://doi.org/10.1016/S0045-7825(97)00075-3)
- Sankar, B.V.: An elasticity solution for functionally graded beams. *Compos. Sci. Technol.* **61**(5), 689–696 (2001). [https://doi.org/10.1016/S0266-3538\(01\)00007-0](https://doi.org/10.1016/S0266-3538(01)00007-0)
- Sarathchandra, D.T., Kanmani Subbu, S., Venkaiah, N.: Functionally graded materials and processing techniques: an art of review. *Mater. Today Proc.* **5**(10), 21328–21334 (2018). <https://doi.org/10.1016/j.matpr.2018.06.536>

- Shafei, E., Faroughi, S., Reali, A.: Geometrically nonlinear vibration of anisotropic composite beams using isogeometric third-order shear deformation theory. *Compos. Struct.* **252**, 112627 (2020). <https://doi.org/10.1016/j.compstruct.2020.112627>
- Şimşek, M.: Fundamental frequency analysis of functionally graded beams by using different higher-order beam theories. *Nucl. Eng. Des.* **240**(4), 697–705 (2010). <https://doi.org/10.1016/j.nucengdes.2009.12.013>
- Şimşek, M.: Bi-directional functionally graded materials (BDFGMs) for free and forced vibration of Timoshenko beams with various boundary conditions. *Compos. Struct.* **133**, 968–978 (2015). <https://doi.org/10.1016/j.compstruct.2015.08.021>
- Şimşek, M., Kocatürk, T., Akbaş, Ş.D.: Dynamic behavior of an axially functionally graded beam under action of a moving harmonic load. *Compos. Struct.* **94**(8), 2358–2364 (2012). <https://doi.org/10.1016/j.compstruct.2012.03.020>
- Sina, S.A., Navazi, H.M., Haddadpour, H.: An analytical method for free vibration analysis of functionally graded beams. *Mater. Des.* **30**(3), 741–747 (2009). <https://doi.org/10.1016/j.matdes.2008.05.015>
- Sofiyev, A.H.: Review of research on the vibration and buckling of the FGM conical shells. *Compos. Struct.* **211**, 301–317 (2019). <https://doi.org/10.1016/j.compstruct.2018.12.047>
- Soldatos, K.P.: A transverse shear deformation theory for homogeneous monoclinic plates. *Acta Mech.* **94**(3), 195–220 (1992). <https://doi.org/10.1007/BF01176650>
- Thai, H.T., Vo, T.P.: Bending and free vibration of functionally graded beams using various higher-order shear deformation beam theories. *Int. J. Mech. Sci.* **62**(1), 57–66 (2012). <https://doi.org/10.1016/j.ijmecsci.2012.05.014>
- Tlidji, Y., Zidour, M., Draiche, K., Safa, A., Bourada, M., Tounsi, A., Bousahla, A.A., Mahmoud, S.R.: Vibration analysis of different material distributions of functionally graded microbeam. *Struct. Eng. Mech.* **69**(6), 637–649 (2019). <https://doi.org/10.12989/SEM.2019.69.6.637>
- Touratier, M.: An efficient standard plate theory. *Int. J. Eng. Sci.* **29**(8), 901–916 (1991). [https://doi.org/10.1016/0020-7225\(91\)90165-Y](https://doi.org/10.1016/0020-7225(91)90165-Y)
- Truong, T.T., Lee, S., Lee, J.: An artificial neural network-differential evolution approach for optimization of bidirectional functionally graded beams. *Compos. Struct.* **233**, 111517 (2020). <https://doi.org/10.1016/j.compstruct.2019.111517>
- Van Do, V.N., Jeon, J.-T., Lee, C.-H.: Dynamic analysis of carbon nanotube reinforced composite plates by using Bézier extraction based isogeometric finite element combined with higher-order shear deformation theory. *Mech. Mater.* **142**, 103307 (2020). <https://doi.org/10.1016/j.mechmat.2019.103307>
- Viet, N.V., Zaki, W., Wang, Q.: Free vibration characteristics of sectioned unidirectional/bidirectional functionally graded material cantilever beams based on finite element analysis. *Appl. Math. Mech.* **41**(12), 1787–1804 (2020). <https://doi.org/10.1007/s10483-020-2664-8>
- Wang, X., Yang, Q., Law, S.-S.: A shear locking-free spatial beam element with general thin-walled closed cross-section. *Eng. Struct.* **58**, 12–24 (2014). <https://doi.org/10.1016/j.engstruct.2013.09.046>
- Wang, Y.Q., Zu, J.W.: Vibration characteristics of moving sigmoid functionally graded plates containing porosities. *Int. J. Mech. Mater. Des.* **14**(4), 473–489 (2018). <https://doi.org/10.1007/s10999-017-9385-2>
- Wang, Y., Zhou, A., Fu, T., Zhang, W.: Transient response of a sandwich beam with functionally graded porous core traversed by a non-uniformly distributed moving mass. *Int. J. Mech. Mater. Des.* **16**(3), 519–540 (2020). <https://doi.org/10.1007/s10999-019-09483-9>
- Wei, D., Liu, Y., Xiang, Z.: An analytical method for free vibration analysis of functionally graded beams with edge cracks. *J. Sound Vib.* **331**(7), 1686–1700 (2012). <https://doi.org/10.1016/j.ijmecsci.2012.05.014>
- Xie, K., Wang, Y., Fu, T.: Nonlinear vibration analysis of third-order shear deformable functionally graded beams by a new method based on direct numerical integration technique. *Int. J. Mech. Mater. Des.* **16**(4), 839–855 (2020). <https://doi.org/10.1007/s10999-020-09493-y>
- Xie, K., Wang, Y., Fan, X., Fu, T.: Nonlinear free vibration analysis of functionally graded beams by using different shear deformation theories. *Appl. Math. Model.* **77**, 1860–1880 (2020). <https://doi.org/10.1016/j.apm.2019.09.024>
- Yongdong, L., Hongcai, Z., Nan, Z., Yao, D.: Stress analysis of functionally gradient beam using effective principal axes. *Int. J. Mech. Mater. Des.* **2**(3), 157–164 (2005). <https://doi.org/10.1007/s10999-006-9000-4>
- Zhang, L., Lin, Q., Chen, F., Zhang, Y., Yin, H.: Micromechanical modeling and experimental characterization for the elastoplastic behavior of a functionally graded material. *Int. J. Solids Struct.* **206**, 370–382 (2020). <https://doi.org/10.1016/j.ijsolstr.2020.09.010>
- Zhang, Y.-W., Chen, W.-J., Ni, Z.-Y., Zang, J., Hou, S.: Supersonic aerodynamic piezoelectric energy harvesting performance of functionally graded beams. *Compos. Struct.* **233**, 111537 (2020). <https://doi.org/10.1016/j.compstruct.2019.111537>
- Zhang, Q., Liu, H.: On the dynamic response of porous functionally graded microbeam under moving load. *Int. J. Eng. Sci.* **153**, 103317 (2020). <https://doi.org/10.1016/j.ijengsci.2020.103317>

Publisher's Note Springer Nature remains neutral with regard to jurisdictional claims in published maps and institutional affiliations.